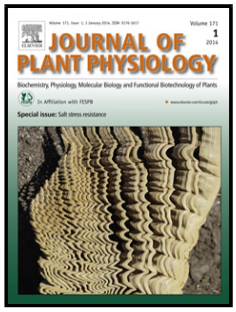

Title: Characterization of *lingering hope*, a new brachytic mutant in sunflower (*Helianthus annuus* L.) with altered salicylic acid metabolism

Authors: Lorenzo Mariotti, Marco Fambrini, Andrea Scartazza, Piero Picciarelli, Claudio Pugliesi

PII: S0176-1617(18)30359-6
DOI: https://doi.org/10.1016/j.jplph.2018.10.020
Reference: JPLPH 52875

To appear in:

Received date: 2-7-2018
Revised date: 2-10-2018
Accepted date: 22-10-2018

Please cite this article as: Mariotti L, Fambrini M, Scartazza A, Picciarelli P, Pugliesi C, Characterization of *lingering hope*, a new brachytic mutant in sunflower (*Helianthus annuus* L.) with altered salicylic acid metabolism, *Journal of Plant Physiology* (2018), https://doi.org/10.1016/j.jplph.2018.10.020

Characterization of *lingering hope*, a new brachytic mutant in sunflower (*Helianthus annuus* L.) with altered salicylic acid metabolism

Running title: A brachytic mutant in sunflower (*Helianthus annuus*)

Lorenzo Mariotti[a,1], Marco Fambrini[a,1], Andrea Scartazza[b], Piero Picciarelli[a], Claudio Pugliesi[a,*]

[a] *Department of Agriculture, Food and Environment, University of Pisa, Via del Borghetto 80, I-56124 Pisa, Italy*

[b] *Institute of Agro-environmental and Forest Biology (IBAF), National Research Council of Italy (CNR), Via Salaria Km 29,300, I-00015 Monterotondo Scalo, RM, Italy*

[1] Lorenzo Mariotti and Marco Fambrini contributed equally to this work

* For correspondence: Claudio Pugliesi, Department of Agriculture, Food and Environment, University of Pisa, Via del Borghetto 80, I-56124 Pisa, Italy

Phone: +39 (0) 50 2216666

Email: claudio.pugliesi@unipi.it

Graphical abstract

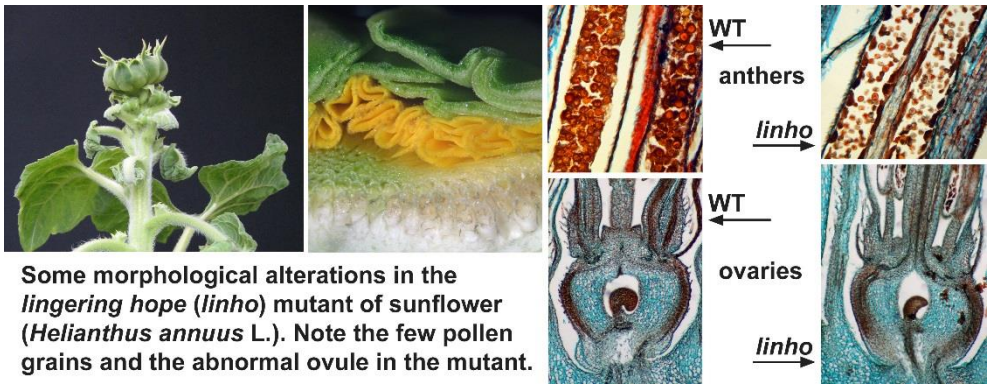

Some morphological alterations in the *lingering hope* (*linho*) mutant of sunflower (*Helianthus annuus* L.). Note the few pollen grains and the abnormal ovule in the mutant.

Original Paper

ABSTRACT

Dwarf mutants are useful to elucidate regulatory mechanisms of plant growth and development. A brachytic mutant, named *lingering hope* (*linho*), was recently isolated from sunflower (*Helianthus annuus*). The aim of this report is the characterization of the mutant through genetic, morphometric, physiological and gene expression analyses. The brachytic trait is controlled by a recessive gene. The reduction of plant height depends on shorter apical internodes. The mutant shows an altered ratio length/width of the leaf blade, chlorosis and defects in inflorescence development. . The brachytic trait is not associated to a specific hormonal deficiency, but an increased level of several gibberellins is detected in leaves. Notably, the endogenous SA content in young leaves of the mutant is very high despite a low level of SA 2-*O*-*β*-D-glucoside (SAG). The CO_2 assimilation rate significantly decreases in the second pair of leaves of *linho*, due to effects of both stomatal and non-stomatal constraints. In addition, the reduction of both actual and potential photochemical efficiency of photosystem II is associated with a reduced content of chlorophylls and carotenoids, a lower chlorophyll *a* to chlorophyll *b* ratio and a higher SA content. In comparison to wild type, *linho* shows a different pattern of gene expression with respect two pathogenesis-related genes and two genes involved in SA biosynthesis and SA metabolism. *linho* is the first mutant described in sunflower with

altered SA metabolism and this genotype could be useful to improve information about the effects of high endogenous content of SA on plant development, reproductive growth and photosynthesis, in a major crop.

Key words: Helianthus annuus, Gibberellins, Indole-3-acetic acid (IAA), Salicylic acid, Gas exchange, Chlorophyll fluorescence, Brachytic mutant.

1. Introduction

Internode elongation of crop stems is one of the most important agronomic traits to ensure lodging resistance and suitable plant architecture for optimising crop performance and yield (Mathan et al., 2016). The control of organ growth is a very complex phenomenon mediated by a plethora of external and internal factors . Among internal factors, gibberellins (GAs) play an essential role in the regulation of plant height . Mutants with a deficiency in GAs concentration or response are frequently dwarf or semi-dwarf, while elevated GAs concentration or increased signalling result in taller plants. Genes coding for proteins implicated in GA metabolic and response have provided the basis of the 'Green Revolution' (Hedden, 2003). However, other hormones as auxin (Multani et al., 2003), brassinosteroid (Fujioka and Yokota, 2003), strigolactones (de Saint Germain et al., 2013) and salicylic acid (Rivas-San Vicente and Plasencia, 2011) are involved in the regulation of plant height.

The development of shorter genotypes is of interest in sunflower breeding because reduction in plant height can led to an improved harvest index and to enhanced lodging resistance under high nitrogen fertilization (Weiss, 2000; Hall et al., 2010). In addition, sunflower varieties would be also used as potted plants for floriculture markets if height could be effectively controlled.

In sunflower, stem length is determined by number and length of internodes (Knowels, 1978). The elongation of internodes starts more rapidly at the base but, successively, it shifts progressively up, while ceased at the base when the internodes reached 60% of their final length. Internode elongation depends by both cell division and cell expansion. More recently, in this crop, the interaction of both light quality and photosynthetically active radiation (PAR) irradiance with several hormones (GAs, cytokinins (CKs), auxin and ethylene) in controlling internodes growth has been established (Kurepin et al., 2007a; b; c). ~~111~~The nomenclature in literature about plants characterized by shortening of the internodes is frequently inappropriate. As pointed out by Cook (1915), the word "brachysm" should be suggested as a name for abnormal variations of plants characterized by shortening of internodes, without corresponding reductions of other parts, while true dwarfing involves proportional diminutions of many parts, if not of all. On the other hand, this classification is not simple to use because accurate analysis can identify pleiotropic phenotypes.

Dwarfism in sunflower is usually controlled by recessive genes but reduction of plant height can be controlled also by dominant or semi-dominant genes (reviewed in Ramos et al., 2013). To date, two mutations that reduce plant stature have been identified at molecular level: a deletion in the *ent-kaurenoic acid oxidase1* (*HaKAO1*) gene sequence (Fambrini et al., 2011) and a point mutation converting a leucine residue in a proline within the conserved DELLA domain (Nelson and Steber, 2016) encoded by the *HaDella1* gene (Ramos et al., 2013). Genetic defects in GA biosynthesis cause severe dwarfism (Fambrini et al., 2011) while t alteration of the DELLA protein constitutively blocks GA signalling and reduces plant height (Ramos et al., 2013) . Therefore, in plant breeding programs, the semi-dominant allele *Rht1* could be interesting to increase stem strength, stand-ability, and yields (Ramos et al., 2013); nevertheless, severe dwarf genotypes as *dw2* mutant (Fambrini et al., 2011) can be useful to investigate relevant biological aspects as recently demonstrated by Atamian and co-workers (2016) for solar tracking in sunflower.

A comprehensive understanding of the genetic control of plant architecture in crops can provide insight into crop domestication history, morphogenesis and development but also adds a foundation for designing efficient breeding strategies to improve crop yield (Busov et al., 2008).

In this study, we report genetic, morphometric, physiological and gene expression analyses, of a spontaneous brachytic mutant in sunflower named *lingering hope* (*linho*).

2. Materials and methods

2.1. Plant material and growth conditions

The sunflower (*Helianthus annuus* L.) mutant *lingering hope* (*linho*) was identified in the inbred line TURF (Department of Agriculture, Food and Environment, Genetic Section, University of Pisa, Italy). Sunflower seeds [wild type (WT) and *linho*] were germinated in Petri dishes on distilled water. Germination took place in a growth chamber in the dark at 23 ± 1 °C. After 3 days, the germinated seeds were transplanted into small plastic pots (50 mL) containing a mixture of soil and sand. Two weeks later, the seedlings were transplanted into larger pots (3 L) containing the same substrate plus a fertilizer (Osmocote14-14-14; Scotts, Marysville, OH, USA). Growth conditions were 25 ± 1 °C and 16 h photoperiod. Irradiation was 200 μmol m^{-2} s^{-1} (photosynthetic photon flux density, PPFD) provided from a mixture of cool-white fluorescent (Philips TLD 30W/33, Philips, Eindhoven, The Netherlands) and mercury-vapour HPI-T 400 W (Philips) lamps. Chemical treatments for preventive plant protection were practised. Trials were carried out during the spring/summer seasons 2013-2014 in experimental fields at the Department of Agriculture, Food and Environment, Experimental Station of Pisa, on a medium fertility and high field capacity soil. Conventional management practices were used (Fambrini et al., 2006). The genetic analysis was

performed by self-pollination of heterozygous plants (*LINHO*/*linho*) because *linho* pollen was infertile and distribution of WT pollen on *linho* stigmas (by hand pollination) did not allow the production of achenes, suggesting the embryo sac sterility.

2.2. In vitro *culture*

Sunflower seeds of homozygous WT (*LINHO*/*LINHO*) and heterozygous (*LINHO*/*linho*) plants were surface-sterilized by immersion into a 70% (v/v) ethanol for 2 min. Successively, the seeds were immersed into a 2.5% (v/v) solution of sodium hypochlorite for 20 min and rinsed four times in sterile distilled water. Afterwards, they were placed in Petri dishes on 25 mL of fourth-strength MS medium (Murashige and Skoog, 1962; pH 5.7) containing 5 g L^{-1} sucrose and 8 g L^{-1} bacteriological agar (Oxoid LTD., Basingstoke, England). The plates were incubated for 7 days at 23 ± 1 °C for germination in a growth chamber under a 16 h light photoperiod with a light intensity of 30 μmol m^{-2} s^{-1}. Each seedling was cut at hypocotyl level and explants were transferred in flask (100 mL) under a 16 h light photoperiod with a light intensity of 30 μmol m^{-2} s^{-1} and grown for three weeks on half-strength MS medium containing 5 g L^{-1} sucrose and 8 g L^{-1} agar. Rooted plants were then photographed.

2.3. Morphological analyses

The height of plants grown in the field was determined from ground to the receptacle, during reproductive stages R3 and R6 (according to Schneiter and Miller, 1981; Table S1). At R 5.6/R6 stage, the total number of leaves was also determined. These observations were made on randomly

selected plants (n = 10) of three replicate progenies of both *linho* and WT. Time-dependent variations of plant height, internode length (from the base of one node to the base of the next node) and total leaf number were determined weekly in both WT and *linho* potted plants. Internodes were numbered from the hypocotyl to the last detectable unit below the inflorescence. Evaluation of these parameters was performed using 10 plants from each genotype. Over 500 leaves (from immature to mature, isolated from 20-30 plants of each genotype) were measured to collect length and width parameters; furthermore, the relative ratio (leaf index) was evaluated. Leaf index, namely, the ratio of leaf length to leaf width is rather stable for a given species (Tsukaya, 2002). Quantitative parameters such as epidermis cell area, palisade cell diameter (determined in a paradermal view), were measured by using digital images of cleared leaf disks (Fambrini et al., 2010) using image analysis software (ImageJ).

2.4. Histological analysis

Shoot tips, segments of leaves (immature and mature), internodes and inflorescence meristems of *linho* and WT plants were collected from potted plants. Explants were collected at different plant ages during both vegetative stages V4-V6 (Schneiter and Miller, 1981) and early reproductive stage R1 (Schneiter and Miller, 1981). Plant material was fixed for 24 h in FAA solution [5% (v/v) acetic acid, 50% (v/v) ethanol, 10% (v/v) formaldehyde, and 35% distilled water], dehydrated using a graded ethanol series, and then cleared in Noxil (Italscientifica S.p.A., Genova, Italy) in a five step-process according to Ruzin (1999). Samples were embedded in Paraplast Plus (Sigma-Aldrich Co. LLC, St. Louis, USA) and sectioned at 8 μm using a manual rotary microtome (Reichert, Vienna, Austria). The serial transverse sections were stained with a solution containing Alcian Blue 8GX, Bismarck Brown Y, and Safranin O according to Graham and Trentham (1998). Sections were

observed with a Leica DMRB light microscope (Leica Microsystems, Wetzlar, Germany) and images were recorded with a digital camera. To determine cell length (μm) in cross and longitudinal sections of eighth-ninth internode of potted plants, slides were observed with a Leica DMRB light microscope (Leica Microsystems) and images were recorded with a digital camera. ImageJ was utilized to collect data.

2.5. Pigment analysis

Spectrophotometric analysis of pigments was performed as previously described (Fambrini et al., 2004). Samples were taken from the first and second pair leaves of 21-day-old WT and *linho* plants grown in a growth chamber. For each genotype ten samples were extracted. The spectrophotometric determinations were made in parallel with two aliquots for each extract.

2.6. Analysis of endogenous hormones

Approximately 1,000 mg of WT and *linho* leaves were extracted and purified as described (Fambrini et al., 2011). To analyse hormonal content, leaves from 21-days-old and 70-days-old plants, were collected. The material was homogenized in cold 80% (v/v) methanol (1:5, w/v) using a microdevice. Deuterated GAs ([17,17-$^{2}H_{2}$]-GA_{19}, [17,17-$^{2}H_{2}$]-GA_{20}, [17,17-$^{2}H_{2}$]-GA_{29}, [17,17-$^{2}H_{2}$]-GA_{1}, [17,17-$^{2}H_{2}$]-GA_{8}, obtained from L. N. Mander, Australian National University, Canberra, Australia), [$^{2}H_{4}$]-SA, [$^{2}H_{5}$]-JA, [$^{2}H_{6}$]- ABA (CDN Isotopes Inc., Quebec, Canada) and [$^{13}C_{6}$]-IAA (Cambridge Isotopes Laboratories Inc., Andover, MA, USA) were added as internal standards to account for purification losses. Methanol was evaporated under vacuum at 35 °C and the aqueous

phase was partitioned against ethyl acetate, after adjusting the pH to 2.8. The extracts were dried and resuspended in 0.3-0.5 mL of water with 0.01% acetic acid and 10% methanol. HPLC analysis was performed with a Kontron instrument (Munich, Germany) equipped with a UV absorbance detector operating at 214 nm. The samples applied to an ODS Hypersil column (150 × 4.6 mm I.D. and 5 μm of a particle size; Thermo) were eluted at a flow rate of 1 mL min^{-1}. The column held constant at 10% MeOH for 5 min of the run, followed by a double gradient elution from 10% to 30% and 30% to 100% over 20 min. The fractions corresponding to the elution volumes of standard hormones were collected separately. The fractions were dried and silylated with N,Obis (trimethylsilyl) trifluoroacetamide containing 1% trimethylchlorosilane (Pierce, Rockford, IL, USA) at 70 °C for 1 h. Chromatography-tandem mass spectrometry (GC-MS/MS) analysis was performed on a Saturn 2200 quadrupole ion trap mass spectrometer coupled to a CP-3800 gas chromatograph (Varian Analytical Instruments, Walnut Creek, CA, USA) equipped with a MEGA 1MS capillary column (30 m × 0.25 mm i.d., 0.25 μm film thickness) (Mega, Milano, Italy). The carrier gas was helium, which was dried and air free, with a linear speed of 60 cm s^{-1}. The oven temperature was maintained at 80 °C for 2 min and increased to 300 °C at a rate of 10 °C min^{-1}. Injector and transfer line were set at 250 °C and the ion source temperature at 200 °C. Full scan mass spectra were obtained in EI+ mode with an emission current of 10 μA and an axial modulation of 4 V. Data acquisitions were from 150 to 600 Da at a speed of 1.4 scan s^{-1}. Final data were the means of three biological replicates. Gibberellins were identified by comparison of full mass spectra with those of authentic compounds. Quantification was carried out by reference to standard plots of concentration ratios versus ion ratios, obtained by analysing known mixtures of unlabeled and labelled GAs.

2.7. Gas exchange and chlorophyll (Chl) fluorescence measurements

Gas exchange and fluorescence measurements were performed using the LI-6400-40 portable photosynthesis system (LI-COR) equipped with the leaf chamber fluorometer (Scartazza et al., 2017). Measurements were carried out on the first and the second pair of leaves from five individual plants of both *linho* and WT. Instantaneous measurements of steady-state photosynthetic CO_2 assimilation rate (A), stomatal conductance (g_s), intercellular CO_2 concentration (C_i), transpiration rate (E), actual photon yield of PSII photochemistry (Φ_{PSII}), Stern–Volmer non-photochemical quenching (NPQ) and potential efficiency of PSII photochemistry (F_v/F_m) were determined between 10:00 and 12:00 h under growing light conditions (200 μmol m^{-2} s^{-1}), CO_2 concentration of 400 μmol mol^{-1}, leaf temperature of 25 °C and relative humidity of 45-55%. Φ_{PSII} was determined at steady state as $\Phi_{PSII} = (F_m - F')/F_m$, where F_m is the maximum fluorescence yield with all PSII reaction centres in the reduced state obtained superimposing a saturating light flash during exposition to actinic light and F' is the fluorescence at the actual state of PSII reaction centres during actinic illumination. NPQ was calculated according to the Stern-Volmer equation as $NPQ= (F_m/F_m')$-1, where F_m is the maximum fluorescence yield in the dark. F_v/F_m was determined on dark-adapted leaves (at least 30 min) as $F_v/F_m= (F_m-F_0)/F_m$, where F_0 is the minimal fluorescence yield emitted by the leaves in the dark-adapted state (Scartazza et al., 2016).

2.8. Gene expression analysis by reverse transcription-quantitative real-time polymerase chain reaction (RT-qPCR)

Expression analysis by RT-qPCRs was performed for genes of sunflower implicated in the response to exogenous SA treatment as well to biotic stress [*Pathogenesis-related 5-1* (*PR5-1*) and *Defensin* (*PDF 1.2*)], SA metabolism [*UDP-glycosyltransferase 74G1-like* (*SA GTase*)] or involved in SA biosynthesis [*Isochorismate synthase 2* (*ICS2*)]. The GenBank accession numbers, the gene-specific primers used for this analysis and the amplicon size are reported in Table S2.

Total RNA was extracted from young leaves (15^{th}/18^{th}) of WT and *linho* plants with the TriPure Isolation Reagent, according to the manufacturer's instructions (Roche Diagnostics GmbH, Mannheim, Germany). Mutant leaves showed folded lamina. Total RNA was treated with DNase I-RNase free (Dasit Sciences S.r.l., Cornaredo, Milan, Italy) as previously described (Fambrini et al., 2018) and retrotranscribed with the iScript™ cDNA synthesis kit, according to the manufacturer's instructions (Bio-Rad Laboratories S.r.l., Segrate, Milan, Italy).

Expression analysis was conducted using a Real-time Step One (Applied Biosystem, Thermo Fisher Scientific Inc., Waltham, MA, USA) and gene-specific primers (Table S2). Quantitative PCR was performed using 12.5 ng of cDNA and PowerUp SYBR Green Master Mix (Thermo Fisher Scientific Inc.), according to the manufacturer's instructions. The thermal cycling conditions of RT-qPCR were as follows: 50 °C for 2 min; 95 °C for 2 min; 40 cycles (95 °C-15 sec, 56 or 57 °C-30 sec, 72 °C 1 min); Melt curve: 95 °C-15s /60° C-15 s/ 95 °C-15s. Relative quantification of specific mRNA levels was performed using the comparative $2^{-\Delta\Delta C}$T method (Livak and Schmittgen, 2001). Briefly, the C_T values of the amplified regions in all samples were normalized with the C_T values of the reference housekeeping gene *18S* mRNA to eliminate the variations caused by sample handling. In addition, mRNAs from WT were used as reference sample. Melt-curve analyses were performed after the PCR. A single distinct peak was observed for each target (*PR5-1*, *PDF 1.2*, *SA GTase* and *ICS2*) and control (*18S*) genes indicating the specific amplification of a single product. *18S* was used as the reference gene based on preliminary data that revealed consistent expression levels regardless of these organ types. In particular, the *18S* was preferred after comparison with other putative housekeeping genes (Fambrini et al., 2018). The data were the average from three-four biological replicates, with each including three technical replicates. The software Real-time Step One v2.3, provided with the instrument by which we carried out the RT-qPCR, was used.

2.9. Statistical analysis

For the genetic analysis we used the chi-square (χ^2) test to determine the goodness-of-fit of our experimental ratios to a 3:1 ratio expected for a trait controlled by a single recessive allele. A homogeneity χ^2 test was used before progenies were pooled. In addition, a statistical analysis was carried out on morpho-physiological parameters. Reported values are means (± SE) from three independent experiments (progenies or plants), with 10-50 replicates each (leaves). Differences between means were tested using the Student's *t*-test ($P = 0.05$ or 0.01). The data presented in Figures 3C and 3D were treated using linear regression analysis. Statistical analyses on percentage data were performed after arcsine transformation. For RT-qPCR, the data ± SD were shown as an average expression value in the three or four biological replicates relative to that in the control sample that was set as one. Student's *t*-test was performed to analyse the differences in gene expression between genotypes and was indicated with (* $P < 0.05$) or (** $\underline{P} < 0.01$) in Figures.

3. Results

3.1 Genetic analysis

Recently, a spontaneous mutant named *lingering hope* (*linho*) was isolated within the inbred line TURF of sunflower, which presents dwarf/brachytic phenotype. The genetic analysis suggested a monogenic control of the mutant phenotype because the segregation of heterozygous progenies, fits the hypothesized 3:1 ratio. The Chi-square test for heterogeneity was also not significant (Table 1).

3.2. Developmental defects of the linho *mutant*

At the cotyledonary stage, within heterozygous progenies, mutant plants were not easily identified. However, when seedlings differentiated the first three/four pairs of leaves, *linho* plantlets were recognizable in field due to smaller size of immature leaves and leaf chlorosis (Fig. 1A). Dwarfism of the mutant in the field became very evident after the transition of the vegetative meristem to the reproductive phase (phase change) (Fig. 1B); in fact, the mutant height at R3 and R6 growth stages (Schneiter and Miller, 1981; Table S1) was clearly reduced respect to WT (Table 2). At reproductive stage, the *linho* mutant also showed immature leaves with folded lamina essentially located underneath the capitulum (Fig. 1C). Moreover, the *linho* mutant developed a small inflorescence with abnormal flowering (Fig. 1D).

To characterize the mutant phenotype, we grown WT and *linho* potted plants in a growth chamber. In a controlled environment, young *linho* plants showed the size of third and fourth leaf pairs like to WT but with chlorosis especially in the proximal end (Figs. 2A-B). After these early phases of vegetative development, the height of *linho* plants was progressively reduced in comparison to WT (Fig. 3A). In fact, during reproductive development, the different height between WT and mutant was evident due to shorter internodes as shown in Figure 3B where internode length was reported from the hypocotyl to the fourteenth internode (see also Figure 2F to compare internode elongation in defoliated plants at reproductive phase). To establish if the observed reduction in internode length of the *linho* mutant was due to differences in cell elongation, we sectioned developing internodes. Surprisingly, the *linho* mutant had no smaller cells than WT (Table S3).

At the reproductive stage, a lower number of leaves was observed in *linho* in comparison to WT plants (Fig. 4A). In potted plants, at the end of life cycle, we observed fewer roots in the mutant in comparison to WT (Fig. 2D); furthermore, the dwarfism of the *linho* mutant was also confirmed *in vitro* on a MS medium with sucrose (Fig. 2E).

From vegetative to reproductive stages, we conducted a wide and detailed analysis of leaf length and leaf width (leaf index) to evaluate the relationship of these morphometric parameters. In *linho* plants, the leaf index was significantly different in comparison to WT (Figs. 3C-D). As previously observed in field conditions, also in potted plants, we confirmed the development of *linho* leaves with folded lamina after the vegetative stage (41.9% in 59-days-old plants), as well as the occasionally differentiation of leaf with a strong asymmetric lamina (Fig. 2C). Cytological analyses demonstrated smaller cells in adaxial and abaxial epidermis as well palisade layer of *linho* leaves in comparison to WT (Fig. 4B). Longitudinal sections of shoot apical meristem (SAM) at vegetative stage, and after vegetative-to-reproductive transition, showed that SAM organization was not impaired in the *linho* mutant (Figs. S1A and S1C). Furthermore, longitudinal sections of *linho* leaves with folded lamina revealed a very immature structure with absence of both palisade and spongy layers (Fig. S1E). However, cross sections through the blade of the fourth *linho* phytomer reveal four distinct tissue layers as well in WT (Fig. S1G).

In the *linho* mutant, the time of phase transition was not significantly different with respect to WT (data not shown); nevertheless, the size of inflorescence was smaller than in WT (Fig. 2F) and exhibited an abnormal orientation (parallel to the ground plane; compare Fig. 5A with Fig. 5B). Flowering process was obstructed by involucral bracts that remained strangely serrated (Figs. 5D-E) and time of start appeared delayed with respect to WT because ray corollas remained compressed below the involucral bracts (Fig. 5E). In the mutant, longitudinal free-hand sections of receptacle also showed the absence, of the medullary cavity (Fig. 5F). Finally, a histological analysis has been conducted to evaluate the development of disc florets in the *linho* in comparison to WT. The organogenesis in the mutant appeared normal (Figs. S2A, S2C, S2D and S2G) but pollen grains differentiation was reduced (Fig. S2I) and ovule shape was abnormal (Fig. S2J).

3.3. Pigments analysis

Pigments analysis were performed in *linho* leaves collected in plant at the vegetative stage. *linho* , especially in the second pair of leaves, were deficient in both chlorophylls and carotenoids content. A reduced ratio between chlorophyll *a* and chlorophyll *b* (Chl*a*/Chl*b*) was also observed (Table 3).

3.4. Gas exchange and Chl fluorescence measurements

To evaluate the effects of the mutation on the photosynthetic performance, gas exchange and fluorescence measurements were performed on the first and second pair of leaves of 21-day-old plants.

The gas exchange parameters determined at growth light intensity (200 μmol m^{-2} s^{-1}) were reported in Table 4. Results indicated the lack of significant differences in all the gas exchange parameters between WT and *linho* mutant in the first pair of leaves, while in the second pair, the *linho* mutant showed a lower *A*, *gs*, and *E* than WT. Conversely, *Ci* did not show any statistically significant difference in both pairs of leaves. Regards the fluorescence parameters a significant reduction of both Φ_{PSII} and F_v/F_m, in the second pair of leaves of *linho* was observed compared to WT, while the first pair of leaves did not show any significant difference. In addition, *NPQ* remained statistically unchanged between *linho* and WT in both the first and the second pair of leaves.

3.5. Hormonal content

The pleiotropic defects observed in *linho* development suggested that hormones are likely involved; hence, to test the hypothesis, we performed in leaves of WT and *linho* mutant, a preliminary

hormonal analysis of the following plant hormones: abscisic acid (ABA), IAA, jasmonic acid (JA), GAs and SA. The hormonal profile evidenced different endogenous amounts of IAA, GAs and SA (Fig. 6). We focused the analysis on these hormonal classes during vegetative stage on first and second pair of leaves (stage V6; Schneiter and Miller, 1981) or reproductive phase on $11^{th}/12^{th}$ leaves, numbered from cotyledons, and in the younger $15^{th}/18^{th}$ leaves (stage R5.3/R5.6; Schneiter and Miller, 1981).

In 21-day-old plants, the SA content in the second pair of leaves of the mutant was near the double of that observed in WT even though, in first pair of leaves, the SA content was higher in the WT (Fig. 6A); moreover, *linho* mutant showed a slight increase of IAA content especially in the second pair of leaves (Fig. 6B). To assess the effect of mutation on endogenous GA content, GAs from the early 13-hydroxylation pathways (GA_{19}, GA_{20}, GA_{29}, GA_1, GA_8) were quantified in the first and in the second pair of leaves. In the first and in the second pairs of leaves the most abundant GAs were GA_{19} and GA_{20} but with an opposite trend. The content of GA_{19} and GA_{20} was higher in WT compared to *linho* . In contrast, in the second pair of leaves GA_{19} was higher in the mutant while the amount of GA_{20} was quite similar in both samples (Figs. 6 C-D). The second pair of *linho* leaves contained higher concentration of the bioactive GA_1 compared to the WT. The contents of GA_{29} (a GA_{20} metabolite) and GA_8 (a GA_1 metabolite) were also higher in *linho* than in WT (Fig. 6D).

In 70-day-old plants, at reproductive stage, we analysed the endogenous content of SA and its predominant inactive conjugate, SA 2-*O*-*β*-D-glucoside (SAG), as well as, IAA and GAs using two groups of leaves: $11^{th}/12^{th}$ leaves and $15^{th}/18^{th}$ leaves. About the latter, mutant leaves showed folded lamina. During the reproductive stage, free SA content of mutant leaves was doubled up in the $15^{th}/18^{th}$ leaves but also significantly higher than in WT, in $11^{th}/12^{th}$ leaves (Fig. 6E) while SAG levels in WT leaves were very high respect to the mutant (Fig. 6F). No significant difference in SA + SAG content was observed (Fig. 6G). In both leaf samples of the mutant predominant GAs were GA_{19}

and GA_8 in comparison with WT (Figs. 6H-I). At reproductive stage, in young and old leaves the level of free IAA was similar in WT and in the *linho* mutant (data not shown).

3.6. Gene expression analysis in folded leaves of linho *mutant and in coeval WT leaves*

To evaluate if the high free SA content of the mutant in the young $15^{th}/18^{th}$ leaves was correlated to a peculiar pattern of gene expression, we analysed by RT-qPCRs, two pathogenesis-related genes (*PR5-1* and *PDF 1.2*), one gene implicated in SA biosynthesis (*ICS2*) and one gene related to SA metabolism (*SA GTase*). *PR5-1* resulted down-regulated in *linho* leaves (Fig. 7A), by contrast, *PDF 1.2*, *ICS2* and *SA GTase* were up-regulated in *linho* leaves in comparison to WT (Figs. 7B-D).

4. Discussion

Here, we described a new recessive sunflower mutation that adversely affects several aspects of plant growth during both vegetative and reproductive stage. A prominent trait of *linho* was the reduced height due to very short internodes mainly at the reproductive stage. Below the inflorescence, the *linho* plants showed a cluster of several stem nodes, while in WT the apical internodes were elongated. Origin of the internodes in sunflower, like in rice, depends on the SAM activity and transition of the SAM from the vegetative to the reproductive stage induces internodes elongation (Yamamuro et al., 2000). With regards to uppermost internode lengths, the *linho* mutant is very dissimilar to other sunflower mutants as *dw2* and *Rht1* (Fambrini et al., 2011; Ramos et al., 2013), while it seems more like 'nl' type of gramineous plants. In some gramineous plants, Takeda (1977) contemplated internode elongation mutants into six groups based on the elongation pattern of the

upper four or five internodes. The 'nl' type shows reduced length of the uppermost internode and increased length of basal internodes (Takeda, 1977).

The reduced height of the *linho* plants also was influenced by a reduced number of phytomeres, evidenced during the reproductive stage but it is necessary to consider that the short uppermost internodes and the very small leaves bordering the inflorescence of the *linho* can hinder the count. Furthermore, in sections of eighth-ninth internodes, no defects in cellular length were observed. Hence, the reduction in internode length in the mutant could be due to a reduced cell proliferation.

In addition to short and solid uppermost internodes, brachytic *linho* showed also defects in leaf and inflorescence development. In *linho* leaves, we observed an alteration of leaf width/length ratio, asymmetric shape and more frequently, undersized lamina curled downwards in uppermost nodes. Inflorescences of *linho* were sterile and smaller than in WT while the flowering process was obstructed by involucral bracts that remained strangely serrated. Developmental defects of the *linho* plants were quite complex and comparable, almost in part, with the phenotype of the *Developmental disaster1* (*Dvd1*) mutant of maize (Phillips et al., 2009). However, *Dvd1* mutants have fewer branches, spikelets, florets, and floral organs in the inflorescence due to defects in axillary meristems (AMs), while in *linho* , AM development was normal (data not shown).

The reduced size of the *linho* mutant could be partly due to the impaired photosynthetic activity evidenced by gas exchange and fluorescence analysis of young plants. The lower CO_2 assimilation rate in *linho* mutant compared to WT was evident starting from the second pair of leaves and was partly attributable to a reduced stomatal conductance. However, despite the partial stomatal closure, *linho* plants did not show any statistical differences in intercellular CO_2 concentration compared to WT, suggesting reduced carboxylation efficiency (Fiorini et al., 2016). Hence, our data highlight that both stomatal and non-stomatal constraints contributed to the reduced photosynthetic performance in the *linho* mutant. This was related to changes in the photosynthetic pigments, with a significant decrease in both chlorophylls and carotenoids in *linho* mutant with respect to WT. The reduction in

pigments concentration was more marked in the second pair of leaves, which showed also a decreased Chl*a*/Chl*b* ratio. Changes in this ratio suggest a modification of the structure and functioning of the photosynthetic apparatus, being Chl*a* mainly localized in the reaction centres and antennae of both photosystems, while Chl*b* is restricted to light harvesting systems (Croce, 2012; Esteban et al., 2015). Hence, a reduction of Chl*a*/Chl*b* ratio could affect the light energy conversion processes at PSII level. In fact, *linho* showed a reduction of both potential (F_v/F_m) and actual (Φ_{PSII}) photochemical efficiency of PSII in the second pair of leaves.

We suggest that hormonal imbalances could be involved in the origin of pleiotropic phenotype showed by the *linho* plants and to evaluate this hypothesis, we analysed the endogenous leaf content of several hormones: SA, GAs and IAA.

SA is a key hormone that plays direct or indirect roles in regulating many aspects of plant growth and development, as well as thermogenesis and disease resistance (Vlot et al., 2009; Klessig et al., 2018). Furthermore, studies with SA-over-accumulating mutants of *A. thaliana* directly showed an influence of SA on plant growth (Janda et al., 2014).

In the second pairs of leaves of the mutant, the endogenous SA content was higher with respect to WT. At reproductive stage, we found a very relevant increase of free SA content (>3000 ng g^{-1} FW) in the mutant leaves with curled phenotype, also in absence of abiotic or biotic stress. However, the inactive conjugate SA 2-*O*-β-D-glucoside (SAG), in $11^{th}/12^{th}$ and $15^{th}/18^{th}$ leaves, was accumulated only in WT. Therefore, the sum of SA + SAG was not significantly different between WT and *linho* plants. With the aim to analyse molecular aspects of SA biosynthesis and metabolism in the *linho* $15^{th}/18^{th}$ leaves, we evaluated the expression level of *ICS2* and *SA GTase* demonstrating that both genes were up-regulated.

SA biosynthesis in plants occurs via two pathways: cinnamate (phenylpropanoid) and isochorismate. Genomic studies in *Arabidopsis* have revealed that the major portion of SA synthesis

befalls via isochorismate pathway (Dempsey et al., 2011). In fact, *Arabidopsis ics1* mutants accumulate very few pathogenesis-induced SA and display decreased disease resistance (reviewed in Dempsey and Klessig, 2017). Null *ics1* mutants still accumulate some SA, suggesting the existence of an enzymatic activity redundant with ICS1; in fact, *ICS2* encodes a functional ICS enzyme targeted to the plastids (Garcion et al., 2008). To date, in the big family of Asteraceae, *ICS* genes have been studied only in safflower during abiotic stress, and SA treatments (Sadeghi et al., 2013). The authors demonstrated that SA treatments at 1 mM were inductive for *Ct-ICS* expression in leaves, while 0.1 mM SA was ineffective (Sadeghi et al., 2013). Analogously, in $15^{th}/18^{th}$ leaves of *linho* the elevated SA endogenous content could be a promotive condition for *ICS2* transcription.

In silico analysis of the sunflower genome identified only two other incomplete sequences in the linkage group 1 and 15 encoding a putative ADC synthase, a chorismate binding enzyme (GenBank accession number, OTG36315.1) and an additional ICS2 isoform (GenBank accession number, NC_035447.19). However, we cannot exclude that other sequences encoding for ICS isoforms, not yet completely defined, could be present in the complex paleopolyploid genome of sunflower (Badouin et al., 2017).

Glucosylation of SA at its hydroxyl group generates SAG that is transported to the vacuole where it serves as a non-toxic long-term storage form (Dempsey et al., 2011; Vaca et al., 2017). In *Arabidopsis*, SA glucose conjugates are formed by two homologous enzymes (UGT74F1 and UGT74F2) that transfer glucose from UDP-glucose to SA (Thompson et al., 2017). *In silico* analysis of *Helianthus annuus* genome identified two *UDP-glycosyltransferase* genes, 74G1 (SA GTase, Table S2) and 74B1 (GenBank accession NC_035447.1) located in the linkage group 9 and 15, respectively (Badouin et al., 2017). A bioinformatic analysis performed by Clustal Omega at the site https://www.ebi.ac.uk/Tools/msa/clustalo/ of the NCBI indicated that the SA GTase (74G1), here analysed, showed a higher amino acid identity to UGT74F1 with respect to UGT74F2 (data not

shown). It has been proposed that UGT74F1 forms SAG, while UGT74F2 forms primarily salicylic acid glucose ester (SGE) (Thompson et al., 2017).

Levels of SAG increase in parallel with free SA levels during the development of systemic acquired resistance, suggesting that SAG may be associated with plant defence mechanisms (Chen et al., 1995; Enyedi et al., 1992). Moreover, a time-dependent increase of SAG content was observed in tobacco leaves SA-infiltrated (Lee and Raskin, 1998). Little is known about the control of genes encoding for UDP-glycosyltransferase. Leaves of *Arabidopsis*, treated with 0.1 mM SA showed an increase of *UGT74F1* expression (Dean and Delaney, 2008). In rice, treatments with chemical inducers of acquired disease resistance or plant defense activators (i.e. probenazole), induce a significantly increase of *OsSGT1* expression ratio, while RNAi-mediated silencing of the *OsSGT1* gene significantly reduced the probenazole-dependent development of resistance against blast disease suggesting that OsSGT1 is a key mediator of development of chemically induced disease resistance (Umemura et al., 2009). The high level of *SA GTase* expression observed in the folded leaves of *linho* mutant could be related to elevated SA content, possibly inducing a detoxification process.

Interestingly, recent findings suggest that SA affects photosynthetic activity (for reviews see Rivas-San Vicente and Plasencia, 2011 and Janda et al., 2014). Our data indicated that the lower photosynthetic activity in the second pairs of leaves of *linho* mutant, during vegetative stage, was associated with higher SA and lower photosynthetic pigment (chlorophylls and carotenoids) contents with respect to WT. Accordingly, previous studies indicated that plants with constitutively high SA levels were characterized by reduced F_v/F_m, Φ_{PSII} and stomatal conductance (Mateo et al., 2006) and that exogenous treatments with high SA concentrations decreased leaf photosynthesis (Janda et al., 2012), reduced both chlorophyll and carotenoid contents (Çag et al., 2009; Habibi and Vaziri, 2017) and changed chloroplast ultrastructure (Uzunova and Popova, 2000), suggesting that controlled SA levels are crucial for optimal photosynthetic performance and growth affecting thylakoid membranes

and the associated light-induced reactions (Rivas-San Vicente and Plasencia, 2011; Janda et al., 2014). Notwithstanding the effects of SA on photosynthesis are still controversial, it has been proposed that above a threshold concentration SA can negatively affect the photosynthetic performance through both direct and indirect effects (Janda et al., 2012; Janda T. et al., 2014). Indeed, SA can have a direct effect on the photosynthetic electron chain by acting on structure and function of PSII centres (Maslenkova et al., 2009), on thylakoid cytochrome f554 level (Sahu et al., 2002) and on thylakoid membrane proteins (Chen et al., 2016); on the other hand, the majority of results suggest that the detrimental effect of high SA concentrations on photosynthesis could be indirect through its action on stomatal closure which may limit the Calvin cycle, leading to an over-reduction of PSII and formation of reactive oxygen species (Janda et al., 2012). However, more studies are needed to further elucidate the stomatal and non-stomatal limitations to photosynthesis in *linho* mutant.

In *Arabidopsis thaliana*, several mutants characterized by abnormal levels of SA have been analysed (reviewed in Rivas-San Vicente and Plasencia, 2011; Ding et al., 2015; Janda and Ruelland, 2015). In this species, is evident that mutations in different genes can induce, directly or indirectly, significant alteration of SA levels. In mutants with reduced SA levels, an increased leaf biomass was frequently observed (Abreu and Munné-Bosch, 2009); by contrast, dwarfism was detected in mutants with SA accumulation in healthy conditions (Vanacker et al., 2001; Song et al., 2004; Janda M. et al., 2014). Moreover, in few cases, dwarfed plants possessed also distorted and curled leaves (Weymann et al., 1995). Interestingly, in mutants such as *constitutive expressor of PR genes* (*cpr 1, 5*) and *lesions simulating disease* (*lsd 6, 7*) characterized by constitutive expression of systemic acquired resistance, the SA and SAG levels were ~30-fold higher than in the WT, like those found in *Arabidopsis* leaves after infection with a necrogenic pathogen (Bowling et al., 1994; Uknes et al., 1993; Weymann et al., 1995). In order to evaluate if *linho* mutant could be a genotype that display constitutive expression of pathogenesis-related genes we detected expression level of *PDF 1.2* and *PR5-1* in $15^{th}/18^{th}$ leaves

characterized by high SA level and low SAG content. We demonstrated that *PDF 1.2* was up-regulated while *PR5-1* was down-regulated. We focused our attention on these two genes because they have been studied in sunflower in some host-pathogen interactions and/or after exogenous SA treatments (Hu et al., 2003; Radwan et al., 2005; Letousey et al., 2007; Şestacova et al., 2016). Therefore, our data suggest that in the *linho* mutant with high SA content, pathogenesis-related genes were differentially expressed.

The endogenous levels of GAs were determined in leaves of both genotypes during the vegetative and reproductive phases of sunflower plants. An increased concentration of several GAs was detected in *linho* mutant leaves. As mentioned above, *linho* leaves development was altered so we suggest that accumulation of GAs may overcome the restraint imposed by the mutation stimulating growth by promoting the destruction of DELLA proteins. In literature it has been clearly demonstrated that reduced GA accumulation causes increased accumulation of DELLAs and consequent growth inhibition while GAs induce their disappearance allowing plant growth (Archard et al., 2006). Evidence of a cross-talk between GAs and SA has been reported in *Arabidopsis* quadruple DELLA mutants (Navarro et al., 2008). In these mutants infected with a biotrophs the SA content was approximately 2-fold higher than in WT. Moreover, several data supported a cross-talk of SA with ABA and GAs during germination (reviewed in Rivas-San Vicente and Plasencia, 2011).

~~3~~Relationship between SA and GA in the regulation of source-sink relation under abiotic stress has been extensively studied (reviewed in Iqbal et al., 2011), while cross-talk between these hormones in flowering control is poorly investigated. GA is the best studied hormone in flowering but an important role in this key phase of plants is played also by other hormones as SA (reviewed in Rivas-San Vicente and Plasencia, 2011; Takeno, 2016; Conti, 2017; Campos-Rivero et al., 2017). Several evidences suggested that the effect on flowering of SA is generally promotive especially under stress conditions (Rivas-San Vicente and Plasencia, 2011; Takeno, 2016); for example, in sunflower, SA treatment induces *HELIANTHUS ANNUUS FLOWERING TIME* (*HAFT*) a key gene that regulates

photoperiod-dependent flower development in different angiosperm species (Dezar et al., 2011; Turck et al., 2008). In the *linho* mutant, timing of floral transition was not influenced by the mutation, but rather, some abnormalities have been observed in inflorescence growth and flower fertility. However, the *linho* inflorescence remains to be characterized about hormonal content and expression profile of genes encoding for transcription factors with relevant roles in flowering process.

In conclusion, the *LINHO* loss of function affects sunflower phenotype, photosynthetic performance and leaf hormonal content but we are aware that, in order to understand the primary effect of mutation, the isolation of the *LINHO* gene will be essential. To the best of our knowledge, *linho* is the first mutant in sunflower with alteration of SA metabolism, in particular SA ratio SAG under non-stress conditions. This mutant could be useful for studying the role of SA in organ morphogenesis, plant growth and flower fertility in relationship with other hormones. Outstanding data on these aspects could be collected, in future investigation, through transcriptome analysis during vegetative and reproductive stage.

CRediT Author Statement

Conceptualization; MF. Data curation; LM, MF, AS, PP, CP. Formal analysis; LM, MF, AS, PP, CP. Funding acquisition; CP, PP. Investigation; LM, MF, AS, PP, CP. Methodology; LM, MF, AS, CP. Supervision; PP. Roles/Writing - original draft; LM, MF, AS, PP, CP. Writing - review & editing; LM, MF, AS, PP, CP.

Acknowledgements

This work was supported by the Special Fund 2017-2018 of the University of Pisa. The funders had no role in study design, data collection and analysis, decision to publish, or preparation of the manuscript.

References

Abreu, M.E., Munne´-Bosch, S., 2009. Salicylic acid deficiency in NahG transgenic lines and *sid2* mutants increases seed yield in the annual plant *Arabidopsis thaliana*. J. Exp. Bot. 60**,** 1261-1271.

Archard, P., Cheng, H., De Grauwe, L., Decat, J., Schoutten, H., Moritz, T., Van Der Straeten, D., Peng, J., Harberd, N.P., 2006. Integration of plant responses to environmentally activated phytohormonal signals. Science 311, 91-94.

Atamian, H.S., Creux, N.M., Brown, E.A., Garner, A.G., Blackman, B.K., Harmer, S.L., 2016. Circadian regulation of sunflower heliotropism, floral orientation, and pollinator visits. Science 353, 587-590.

Badouin, H., Gouzy, J., Grassa, C.J., Murat, F., Staton, S.E., Cottret, L., Lelandais-Brière, C., Owens, G.L., Carrère, S., Mayjonade, B., Legrand, L., Gill, N., Kane, N.C., Bowers, J.E., Hubner, S., Bellec, A., Bérard, A., Bergès, H., Blanchet, N., Boniface, M.C., Brunel, D., Catrice, O, Chaidir, N., Claudel, C., Donnadieu, C, Faraut, T., Fievet, G., Helmstetter, N., King, M., Knapp, S.J., Lai, Z, Le Paslier, M.C., Lippi, Y., Lorenzon, L., Mandel, J.R., Marage, G., Marchand, G., Marquand, E., Bret-Mestries, E., Morien, E., Nambeesan, S., Nguyen, T., Pegot-Espagnet, P., Pouilly, N., Raftis, F., Sallet, E., Schiex, T., Thomas, J., Vandecasteele, C., Varès, D., Vear, F., Vautrin, S., Crespi, M., Mangin, B., Burke, J.M., Salse, J., Muños, S., Vincourt, P., Rieseberg, L.H., Langlade, N.B., 2017. The sunflower genome provides insights into oil metabolism, flowering and Asterid evolution. Nature 546, 148-152.

Bowling, S.A., Guo, A., Cao, H., Gordon, A.S., Klessig, D.F., Dong, X., 1994. A mutation in Arabidopsis that leads to constitutive expression of systemic acquired resistance. Plant Cell 6, 1845-1857.

Busov, V.B., Brunner, A.M., Strauss, S.H., 2008. Genes for control of plant stature and form. New Phytol. 177, 589-607.

Çag, S., Cevahir-Öz, G., Sarsag, M., Gören-Saglam, N., 2009. Effect of salicylic acid on pigment, protein content and peroxidase activity in excised sunflower cotyledons. Pak. J. Bot. 41, 2297-2303.

Campos-Rivero, G., Osorio-Montalvo, P., Sánchez-Borges, R., Us-Camas,, R., Duarte-Aké, F., De-la-Peña, C., 2017. Plant hormone signaling in flowering: An epigenetic point of view. J. Plant Physiol. 214, 16-27.

Chen, Y.E., Cui, J.M., Li, G.X., Yuan, M., Zhang, Z.W., Yuan, S., Zhang, H.Y., 2016. Effect of salicylic acid on the antioxidant system and photosystem II in wheat seedlings. Biol. Plant. 60, 139-147.

Chen, Z., Malamy, J., Henning, J., Conrath, U., Sanchez-Casas, P., Silva, H., Ricigliano, J., Klessig, K., 1995. Induction, modification, and transduction of the salicylic acid signal in plant defense responses. Proc. Natl Acad. Sci. USA 92, 4134-4137.

Cook, O.F., 1915. Brachysm, a hereditary deformity of cotton and other plants. J. Agr. Res. 3, 387-399.

Conti, L., 2017. Hormonal control of the floral transition: Can one catch them all? Dev. Biol. 430, 288-301.

Croce, R., 2012. Chlorophyll-binding proteins of higher plants and cyanobacteria, in: Eaton-Rye, J.J., Tripathy, B.C., Sharkey, T.D. (Eds.), Photosynthesis: Plastid Biology, Energy Conversion and

Carbon Assimilation, Advances in Photosynthesis and Respiration. Springer, Dordrecht, pp. 127-149.

Dean, J.V., Delaney, S.P., 2008. Metabolism of salicylic acid in wild-type, *ugt74f1* and *ugt74f2* glucosyltransferase mutants of *Arabidopsis thaliana*. Physiol. Plant. 132, 417-425.

Dempsey, D.A., Klessig, D.F., 2017. How does the multifaceted plant hormone salicylic acid combat disease in plants and are similar mechanisms utilized in humans? BMC Biol. 23;15(1):23.

Dezar, C.A., Giacomelli, J.I., Manavella, P.A., Ré, D.A., Alves-Ferreira, M., Baldwin, I.T., Bonaventure, G., Chan, R.L., 2011. HAHB10, a sunflower HD-Zip II transcription factor, participates in the induction of flowering and in the control of phytohormone-mediated responses to biotic stress. J. Exp. Bot. 62:1061-1076.

Ding, Y., Shaholli, D., Mou, Z., 2015. A large-scale genetic screen for mutants with altered salicylic acid accumulation in Arabidopsis. Front. Plant Sci. 5, 763.

Ding, Y., Zhao, J., Nie, Y., Fan, B., Wu, S., Zhang, Y., Sheng, J., Zhao, R., Tang, X., 2016. Salicylic-acid-induced chilling- and oxidative-stress tolerance in relation to gibberellin homeostasis, C-Repeat/Dehydration-Responsive element binding factor pathway, and antioxidant enzyme systems in cold-stored tomato fruit. J. Agr. Food Chem. 64, 8200-8206.

de Saint Germain, A., Ligerot, Y., Dun, E.A., Pillot, J.P., Ross, J.J., Beveridge, C.A., Rameau, C., 2013. Strigolactones stimulate internode elongation independently of gibberellins. Plant Physiol. 163, 1012-1025.

Enyedi, A.J., Yalpani, N., Silverman, P., Raskin, I., 1992. Localization, conjugation, and function of salicylic acid in tobacco during the hypersensitive reaction to tobacco mosaic virus. Proc. Natl. Acad. Sci. USA 89, 2480-2484.

Esteban, R., Barrutia, O., Artetxe, U., Fernández- Marín, B., Hernández, A., García- Plazaola, J.I., 2015. Internal and external factors affecting photosynthetic pigment composition in plants: a meta- analytical approach. New Phytol. 206, 268-280.

Fambrini, M., Castagna, A., Dalla Vecchia, F., Degl'Innocenti, E., Ranieri, A., Vernieri, P., Pardossi, A., Guidi, L., Rascio, N., Pugliesi C., 2004. Characterization of a pigment-deficient mutant of sunflower (*Helianthus annuus* L.) with abnormal chloroplast biogenesis, reduced PS II activity and low endogenous level of abscisic acid. Plant Sci. 167, 79-89.

Fambrini, M., Bonsignori, E., Rapparini, F., Cionini, G., Michelotti, V., Bertini, D., Baraldi, R., Pugliesi, C., 2006. *stem fasciated*, a recessive mutation in sunflower (*Helianthus annuus*), alters plant morphology and auxin level. Ann. Bot. 98, 715-730.

Fambrini, M., Degl'Innocenti, E., Guidi, L., Pugliesi, C., 2010. The dominant *Basilicum Leaf* mutant of sunflower controls leaf development multifariously and modifies the photosynthetic traits. Flora 205, 853-861.

Fambrini, M., Mariotti, L., Parlanti, S., Picciarelli, P., Salvini, M., Ceccarelli, N., Pugliesi, C., 2011. The extreme dwarf phenotype of the GA-sensitive mutant of sunflower, *dwarf2*, is generated by a deletion in the *ent-kaurenoic acid oxidase1* (*HaKAO1*) gene sequence. Plant Mol. Biol. 75, 431-450.

Fambrini, M., Salvini, M., Pugliesi, C., 2017. Molecular cloning, phylogenetic analysis, and expression patterns of *LATERAL SUPPRESSOR-LIKE* and *REGULATOR OF AXILLARY MERISTEM FORMATION-LIKE* genes in sunflower (*Helianthus annuus* L.). Dev. Gen. Evol. 227, 159-170.

Fambrini, M., Bellanca, M., Costa Muñoz, M., Usai, G., Cavallini, A., C. Pugliesi, C., 2018. Ligulate inflorescence of *Helianthus* × *multiflorus*, cv. Soleil d'Or, correlates with a misregulation of a

CYCLOIDEA gene characterized by insertion of a transposable element. Plant Biol., doi:10.1111/plb.12876.

Fiorini, L., Guglielminetti, L., Mariotti, L., Curadi, M., Picciarelli, P., Scartazza, A., Sarrocco, S., Vannacci, G., 2016. *Trichoderma harzianum* T6776 modulates a complex metabolic network to stimulate tomato cv. Micro-Tom growth. Plant Soil 400, 351-366.

Fujioka, S., Yokota, T., 2003. Biosynthesis and metabolism of brassinosteroids. Annu. Rev. Plant Biol. 54, 137-164.

Garcion, C., Lohmann, A., Lamodière, E., Catinot, J., Buchala, A., Doermann, P., Métraux, J.P., 2008. Characterization and biological function of the *ISOCHORISMATE SYNTHASE2* gene of Arabidopsis. Plant Physiol. 147, 1279-1287.

Graham, E.T., Trentham, W.R., 1998. Staining paraffin extracted, alcohol rinsed and air dried plant tissue with an aqueous mixture of three dyes. Biotech. Histochem. 73, 178-185.

Habibi, G., Vaziri, A., 2017. High salicylic acid concentration alters the electron flow associated with photosystem II in barley. Acta agric. Slov. 109, 393-402.

Hall, A.J., Sposaro, M.M., Chimenti, C.A., 2010. Stem lodging in sunflower: variations in stem failure moment of force and structure across crop population densities and post-anthesis developmental stages in two genotypes of contrasting susceptibility to lodging. Field Crop Res. 116, 46-51.

Hedden, P., 2003. The genes of the green revolution. Trends Genet. 19, 5-9.

Hu, X., Bidney, D.L., Yalpani, N., Duvick, J.P., Crasta, O., Folkerts, O., Lu, G., 2003. Overexpression of a gene encoding hydrogen peroxide-generating oxalate oxidase evokes defense responses in sunflower. Plant Physiol. 133, 170-181.

Iqbal, N., Nazar, R., Khan, M., Iqbal, R., Masood, A., Khan, N.A., 2011. Role of gibberellins in regulation of source–sink relations under optimal and limiting environmental conditions. Current Sci. 100, 998-1007.

Janda, K., Hideg, É., Szalai, G., Kovács, L., Janda, T., 2012. Salicylic acid may indirectly influence the photosynthetic electron transport. J. Plant Physiol. 169, 971-978.

Janda, M., Šašek, V., Ruelland, E., 2014. The Arabidopsis *pi4kIIIβ1β2* double mutant is salicylic acid-overaccumulating: a new example of salicylic acid influence on plant stature. Plant Signal. Behav. 9, e977210.

Janda, M., Ruelland, E., 2015. Magical mystery tour: salicylic acid signalling. Env. Exp. Bot. 114, 117-128.

Janda, T., Gondor, O.K., Yordanova, R., Szalai, G., Pál, M., 2014. Salicylic acid and photosynthesis: signalling and effects. Acta Physiol. Plant. 36, 2537-2546.

Klessig, D.F., Choi, H.W., Dempsey, D.A., 2018. Systemic acquired resistance and salicylic acid: past, present, and future. Mol. Plant Microbe Interact. 31, 871-888.

Knowels, P.F., 1978. Morphology and anatomy, in: Carter, J.F. (Ed.), Sunflower Science and Technology. American Society of Agronomy, Madison, Wisconsin, pp. 55-87.

Kurepin, L.V., Emery, R.J.N., Pharis, R.P., Reid, D.M., 2007a. The interaction of light quality and irradiance with gibberellins, cytokinins and auxin in regulating growth of *Helianthus annuus* hypocotyls. Plant Cell Env. 30, 147-155.

Kurepin, L.V., Emery, R.J.N., Pharis, R.P., Reid, D.M., 2007b. Uncoupling light quality from light irradiance effects in *Helianthus annuus* shoots: putative roles for plant hormones in leaf and internode growth. J. Exp. Bot. 58, 2145-2157.

Kurepin, L.V., Walton, L.J., Reid, D.M., 2007c. Interaction of red to far red light ratio and ethylene in regulating stem elongation of *Helianthus annuus*. Plant Growth Regul. 51, 53-61.

Lee, H.I., Raskin, I., 1998. Glucosylation of salicylic acid in *Nicotiana tabacum* cv. Xanthi-nc. Phytopathology 88, 692-697.

Letousey, P., de Zélicourt, A., Vieira Dos Santos, C., Thoiron S., Monteau, F., Simier, P., Thalouarn, P., Delevault, P., 2007. Molecular analysis of resistance mechanisms to *Orobanche cumana* in sunflower. Plant Pathol. 56, 536-546.

Livak, K.J., Schmittgen, T.D., 2001. Analysis of relative gene expression data using real-time quantitative PCR and the $2^{-\Delta\Delta CT}$ method. Methods 25, 402-408.

Maslenkova, L., Peeva, V., Stojnova, Z., Popova, L., 2009. Salicylic acid induced changes in photosystem II reactions in barley plants. Biotechnol. Biotechnol. Equip. 23, 297-300.

Mateo, A., Funck, D., Mühlenbock, P., Kular, B., Mullineaux, P.M., Karpinski, S., 2006. Controlled levels of salicylic acid are required for optimal photosynthesis and redox homeostasis. J. Exp. Bot. 57, 1795-1807.

Mathan, J., Bhattacharya, J., Ranjan, A., 2016. Enhancing crop yield by optimizing plant development features. Development 134, 3283-3294.

Multani, D.S., Briggs, S.P., Chamberlin, M.A., Blakeslee, J.J., Murphy, A.S., Johal, G.S., 2003. Loss of an MDR transporter in compact stalks of maize *br2* and sorghum *dw3* mutants. Science 302, 81-84.

Murashige, T., Skoog, F., 1962. A revised medium for rapid growth and bioassays with tobacco tissue cultures. Physiol. Plant. 15, 473-497.

Navarro, L., Bari, R., Achard, P., Lisón, P., Nemri, A., Harberd, N.P., Jones, J.D., 2008. DELLAs control plant immune responses by modulating the balance of jasmonic acid and salicylic acid signaling. Curr. Biol. 18, 650-655.

Nelson, S.K., Steber, C.M., 2016. Gibberellin hormone signal perception: down-regulating DELLA repressors of plant growth and development, in: Hedden, P., Stephen, G.T. (Eds.), The Gibberellins. Annual Plant Reviews, Volume 49. Wiley-Blackwell, Hoboken, NJ, pp. 153-188.

Phillips, K.A., Skirpan, A.L., Kaplinsky, N.J., McSteen, P., 2009. *Developmental disaster1*: A novel mutation causing defects during vegetative and inflorescence development in maize (*Zea mays*, Poaceae). Am. J. Bot. 96, 420-430.

Radwan, O., Mouzeyar, S., Venisse, J.S., Nicolas, P., Bouzidi, M.F., 2005. Resistance of sunflower to the biotrophic oomycete *Plasmopara halstedii* is associated with a delayed hypersensitive response within the hypocotyls. J. Exp. Bot. 56, 2683-2693.

Ramos, M.L., Altieri, E., Bulos, M., Sala, C.A., 2013. Phenotypic characterization, genetic mapping and candidate gene analysis of a source conferring reduced plant height in sunflower. Theor. Appl. Genet. 126, 251-263.

Rivas-San Vicente, M., Plasencia, J., 2011. Salicylic acid beyond defence: its role in plant growth and development. J. Exp. Bot. 62, 3321-3338.

Ruzin, S.E., 1999. Plant Microtechnique and Microscopy. Oxford University Press, New York, Oxford.

Sadeghi, M., Dehghan, S., Fischer, R., Wenzel, U., Vilcinskas, A., Kavousi, H.R., Rahnamaeian, M., 2013. Isolation and characterization of isochorismate synthase and cinnamate 4-hydroxylase during salinity stress, wounding, and salicylic acid treatment in *Carthamus tinctorius*. Plant Signal. Behav. e27335.

Sahu, G.K., Kar, M., Sabat, S.C., 2002. Electron transport activities of isolated thylakoids from wheat plants grown in salicylic acid. Plant Biol. 4, 321-328.

Scartazza, A., Di Baccio, D., Bertolotto, P., Gavrichkova, O., Matteucci, G., 2016. Investigating the European beech (*Fagus sylvatica* L.) leaf characteristics along the vertical canopy profile: leaf structure, photosynthetic capacity, light energy dissipation and photoprotection mechanisms. Tree Physiol. 36, 1060-1076.

Scartazza, A., Picciarelli, P., Mariotti, L., Curadi, M., Barsanti, L., Gualtieri, P., 2017. The role of *Euglena gracilis* paramylon in modulating xylem hormone levels, photosynthesis and water-use efficiency in *Solanum lycopersicum* L. Physiol. Plant. 161, 486-501.

Schneiter, A.A., Miller, J.F., 1981. Description of sunflower growth stages. Crop Sci. 21, 901-903.

Şestacova, T., Giscă, I., Cucereavîi, A., Port, A., Duca, M., 2016. Expression of defence-related genes in sunflower infected with broomrape. Biotechnol. Biotechnol. Equip. 30, 685-691.

Song, J.T., Lu, H., Greenberg, J.T., 2004. Divergent roles in *Arabidopsis thaliana* development and defense of two homologous genes, *ABERRANT GROWTH AND DEATH2* and *AGD2-LIKE DEFENSE RESPONSE PROTEIN1*, encoding novel aminotransferases. Plant Cell 16, 353-366.

Takeda, K., 1977. Internode elongation and dwarfism in some gramineous plants. Gamma Field Symp. 16, 1-18.

Takeno, K., 2016. Stress-induced flowering: the third category of flowering response. J. Exp. Bot. 67, 4925-4934.

Thompson, A.M.G., Iancu, C.V., Neet, K.E., Dean, J.V., Choe, J-y., 2017. Differences in salicylic acid glucose conjugations by UGT74F1 and UGT74F2 from *Arabidopsis thaliana*. Sci. Rep. 7, 46629.

Tsukaya, H., 2002. The leaf index: heteroblasty, natural variation, and genetic control of polar processes of leaf expansion. Plant Cell Physiol. 43, 372-378.

Turck, F., Fornara, F., Coupland, G., 2008. Regulation and identity of florigen: FLOWERING LOCUS T moves center stage. Annu. Rev. Plant Biol. 59, 573-594.

Uknes, S., Winter, A.M., Delaney, T., Vernooij, B., Morse, A., Friedrich, L., Nye, G., Potter, S., Ward, E., Ryals, J., 1993. Biological induction of systemic acquired resistance in *Arabidopsis*. Mol. Plant Microbe Interact. 6, 692-698.

Umemura, K., Satou, J., Iwata, M., Uozumi, N., Koga, J., Kawano, T., Koshiba, T., Anzai, H., Mitomi, M., 2009. Contribution of salicylic acid glucosyltransferase, *OsSGT1*, to chemically induced disease resistance in rice plants. Plant J. 57, 463-472.

Uzunova, A.N., Popova, L.P., 2000. Effect of salicylic acid on leaf anatomy and chloroplast ultrastructure of barley plants. Photosynthetica 38, 243-250.

Vaca, E., Behrens, C., Theccanat, T., Choe, J.Y., Dean, J.V., 2017. Mechanistic differences in the uptake of salicylic acid glucose conjugates by vacuolar membrane-enriched vesicles isolated from *Arabidopsis thaliana*. Physiol. Plant. 161, 322-338.

Vanacker, H., Lu, H., Rate, D.N., Greenberg, J.T., 2001. A role for salicylic acid and NPR1 in regulating cell growth in Arabidopsis. Plant J. 28, 209-216.

Vlot, A.C., Dempsey, D.A., Klessig, D.F., 2009. Salicylic acid, a multifaceted hormone to combat disease. Annu. Rev. Phytopathol. 47, 177-206.

Weymann, K., Hunt, M., Uknes, S., Neunschwander, U., Lawton, H., Steiner, H.Y., Ryals, J., 1995. Suppression and restoration of lesion formation in Arabidopsis *lsd* mutants. Plant Cell 7, 2013-2022.

Weiss, E.A., 2000. Oilseed Crops, Second ed. Blackwell, London.

Winkler, R., Helentjaris, T., 1995. The maize *Dwarf3* gene encodes a cytochrome P450-mediated early step in gibberellin biosynthesis. Plant Cell 7, 1307-1317.

Yamamuro, C., Ihara, Y., Wu, X., Noguchi, T., Fujioka, S., Takatsuto, S., Ashikari, M., Kitano, H., Matsuoka, M., 2000. Loss of function of a rice *brassinosteroid insensitive1* homolog prevents internode elongation and bending of the lamina joint. Plant Cell 12, 1591-1606.

Appendix A. Supplementary data associated with this article can be found in Table S1, Table S2, Table S3, Fig. S1, and Fig. S2.

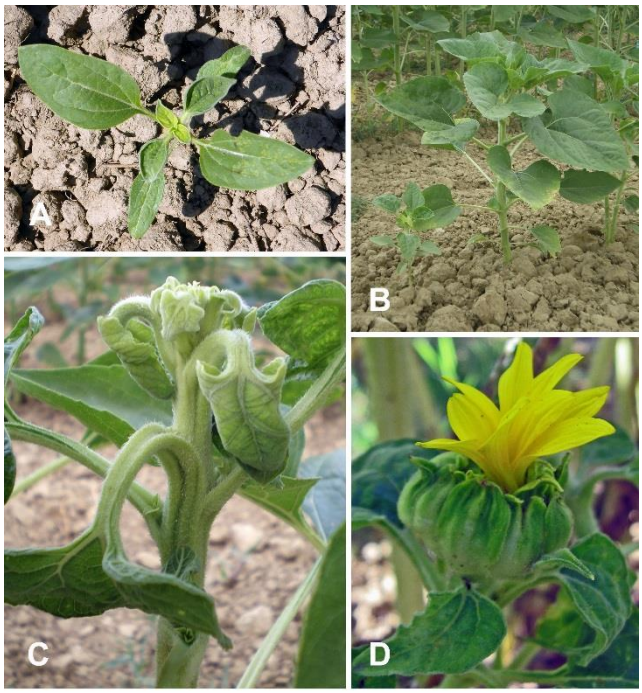

Fig. 1.

Fig. 1. Phenotypic traits showed by the *lingering hope* (*linho*) mutant of sunflower (*Helianthus annuus*) grown in field. (A) A young plant of *linho* (*linho*/*linho*) showing the first signals of developmental defects on younger leaf pairs. (B) Comparison of plant size between wild type (*LINHO*/*LINHO*; WT) (right) and *linho* (left) at early stage of the reproductive phase. (C) Lamina and petiole folded down in *linho* leaves in the reproductive phase. (D) Anthesis in a *linho* inflorescence. Flowering process in the mutant is obstructed by extremely tight involucral bracts. Note only few ray flower corollas that emerge from the centre of capitulum.

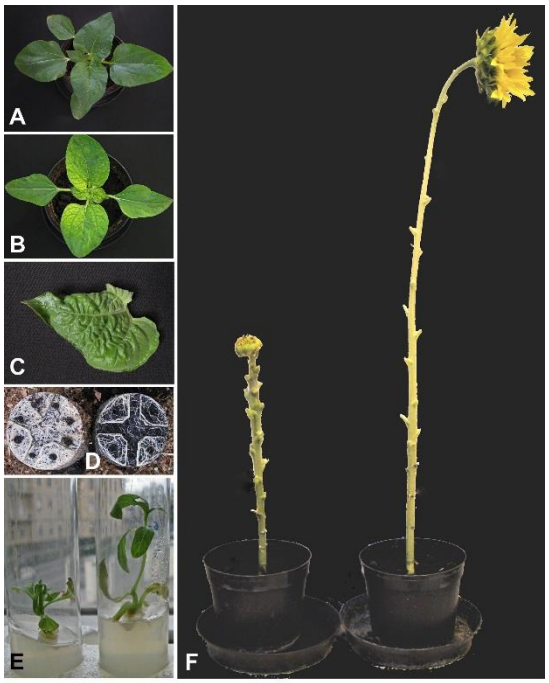

Fig. 2.

Fig. 2. Plants of the *linho* mutant grown in pots and/or *in vitro*. (A) Wild type (*LINHO*/*LINHO*; WT) during vegetative phase. (B) The *linho* mutant (*linho*/*linho*) during vegetative phase. Note interveinal chlorosis at proximal end of younger leaves. (C) Example of a *linho* leaf with asymmetric lamina. (D) Roots of WT (left) and *linho* (right) plants, developed in pots, at the end of life cycle. (E) A *linho* (left) and a WT (right) plantlet growth *in vitro* on solid medium with sucrose. (F) *linho* (left) and WT (right) plants defoliated at reproductive phase to compare internode elongation. Note the cluster of several short internodes just below the *linho* inflorescence.

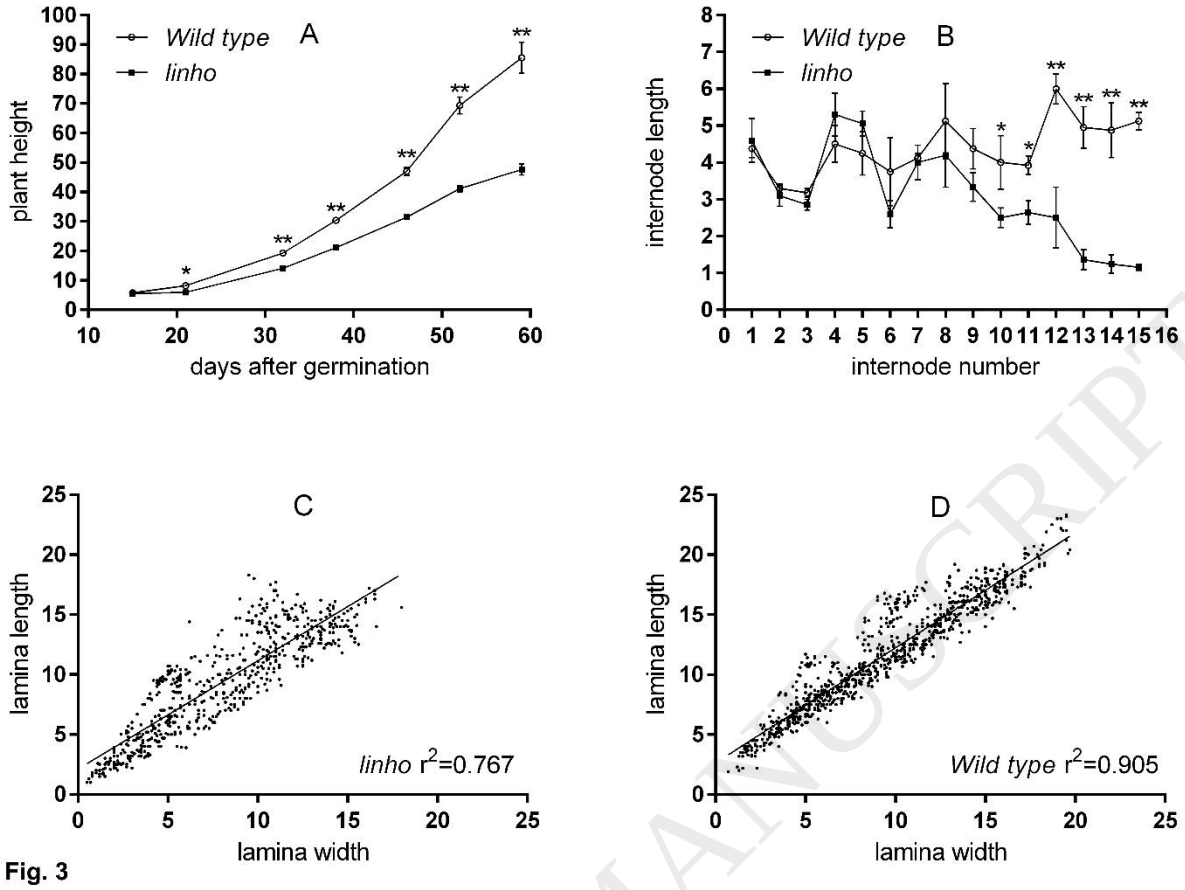

Fig. 3

Fig. 3. Morphometric analysis in wild type (*LINHO*/*LINHO*; WT) and *linho* (*linho*/*linho*) potted plants. (A) Time-dependent increase of plant height (cm) in potted plants of WT and *linho*. (B) Internode length (cm), numbered from cotyledons, in WT and *linho* potted plants measured at 60 days after germination. (C-D) Relationship between length and width (leaf index) of *linho* (C) and WT (D) potted plants. In A and B the data are means of three-four independent experiments (progenies), each with 10 replicate (plants). * Significantly different from WT at the $P < 0.05$ level and ** significantly different from WT at the $P < 0.01$ level, according to a Student's t-test. Data presented in C and D, were treated using linear regression analysis with 10-20 replicate (plants).

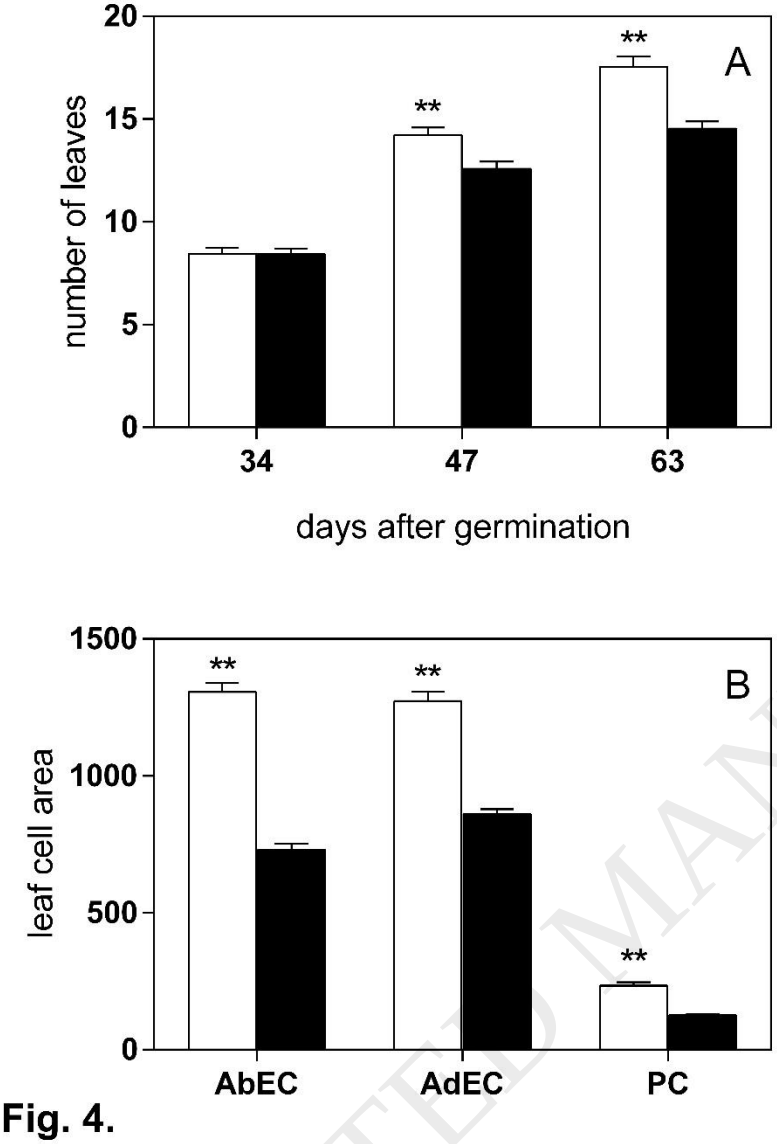

Fig. 4.

Fig. 4. Time-depending increase of leaf number and leaf cell area in wild type (*LINHO*/*LINHO*; WT) and *lingering hope* (*linho*/*linho*) mutant. (A) Number of leaves potted plants at different days after germination. The data are means of three-four independent experiments (progenies), each with 50 replicate (plants). ns: Not significant. ** Significantly different from WT at the $P < 0.01$ level according to a Student's *t*-test. (B) Leaf cell area analysed in clarified disc lamina of leaves from fifth node. Data are means of 5 leaves from 5 potted plants. ** Significantly different from WT at the $P < 0.01$ level according to a Student's *t*-test.

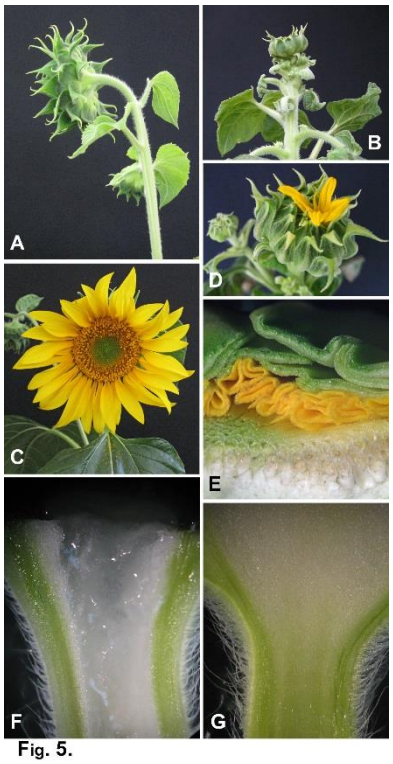

Fig. 5.

Fig. 5. Phenotypic traits of *linho* (*linho*/*linho*) and wild type (*LINHO*/*LINHO*; WT) potted plants at reproductive stage. (A) Vertical orientation of WT inflorescence in growth chamber. (B) Horizontal orientation of the *linho* inflorescence in growth chamber. (C-D) Inflorescence of WT (C) and *linho* (D) at anthesis. (E) Longitudinal free-hand section of the *linho* inflorescence to show the severe compression of ray flower corollas under involucral bracts. (F) Longitudinal free-hand section of WT receptacle with medullary cavity. (G) Longitudinal free-hand section of solid *linho* receptacle.

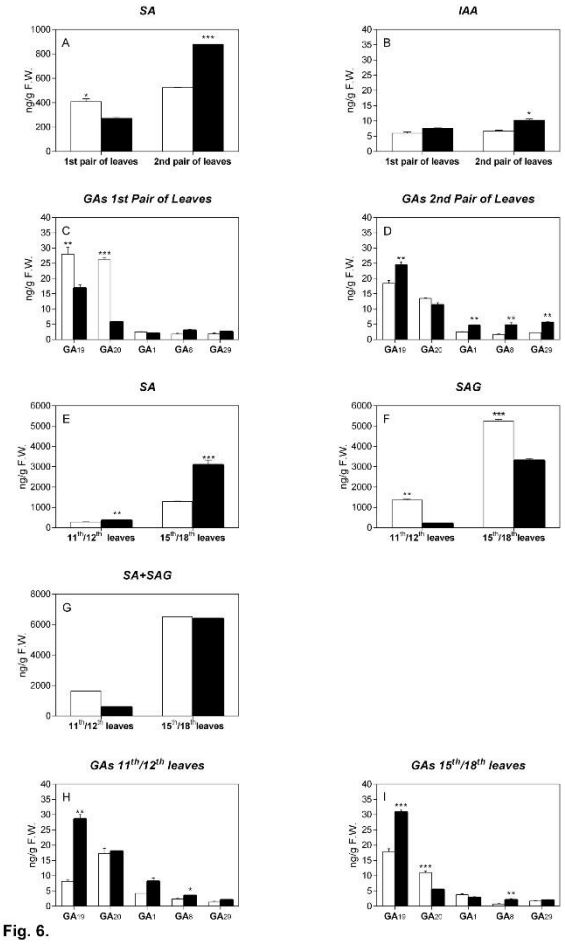

Fig. 6.

Fig. 6. Hormonal analysis in leaves of wild type (*LINHO*/*LINHO*; WT) (white column) and *linho* (*linho*/*linho*) (black column) at different stage of development. 1st and 2nd pair of leaves were analysed from 21-day-old plants, while 11th/12th or 15th/18th leaves, were analysed from 70-day-old plants. Data are endogenous levels (ng g^{-1} fresh weight). (A) Salicylic acid (SA) content in 1st and 2nd pair of leaves of WT and *linho*. (B) Indolacetic acid (IAA) content in 1st and 2nd pair of leaves of WT and *linho*. (C-D) Various gibberellins (GAs) in 1st pair of WT and *linho* (C), or in 2nd pair of leaves (D). (E) SA content in 11th/12th or 15th/18th leaves of WT and *linho*. (F) SA 2-*O*-*β*-D-glucoside (SAG) content in 11th/12th or 15th/18th leaves of WT and *linho*. (G) SA + SAG content in 11th/12th or 15th/18th leaves of WT and *linho*. (H) Various GAs in 11th/12th leaves of WT and *linho*. (I) Various GAs in 15th/18th leaves of WT and *linho*. Data are the mean of three pooled replicates ± SD. Asterisks indicate significant differences between wild type and *linho* mutant (Student't test, *P< 0.05, **P<0.01 or ***P<0.001).

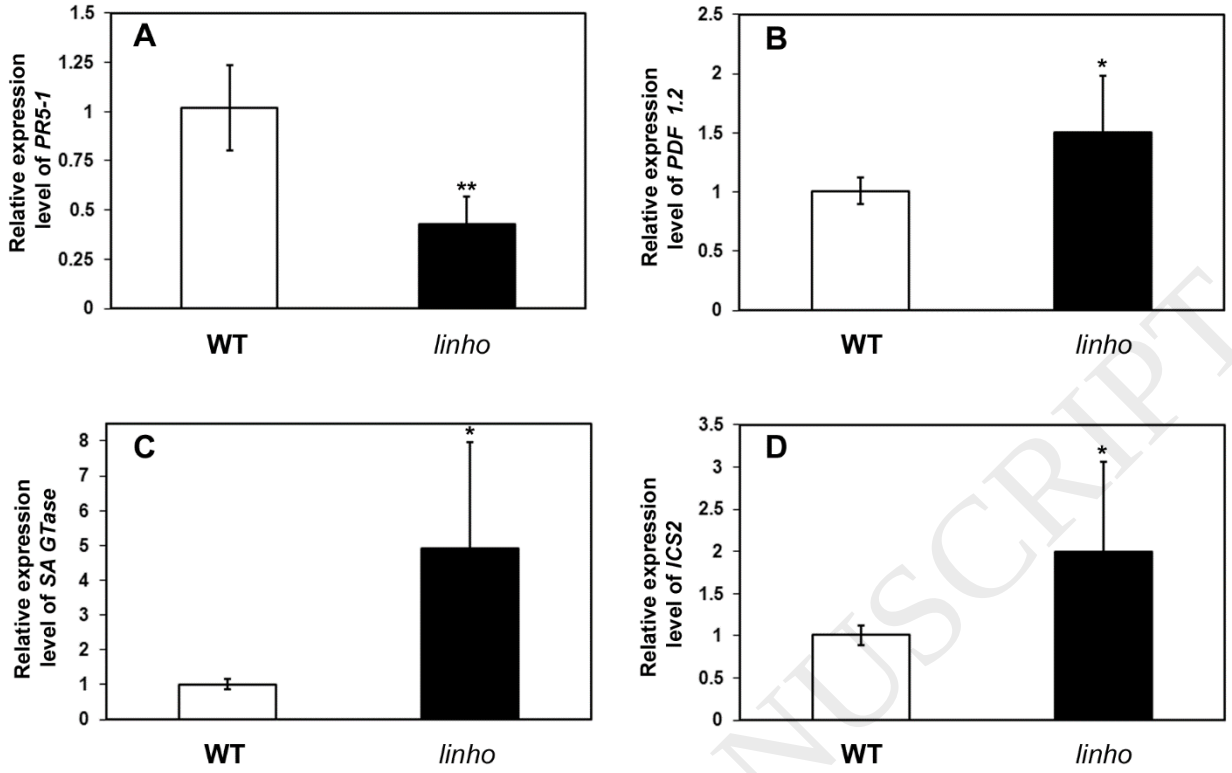

Fig. 7.

Fig. 7. Expression level for genes of sunflower implicated in the response to exogenous SA treatment as well to biotic stress [*Pathogenesis-related 5-1* (*PR5-1*) *Defensin* (*PDF 1.2*)], involved in SA biosynthesis [*Isochorismate synthase 2* (*ICS2*)] or in SA metabolism [*UDP-glycosyltransferase 74G1-like* (*SA GTase*)], in young leaves (15^{th}/18^{th}) of wild type (*LINHO*/*LINHO*; WT) and *linho* (*linho*/*linho*) plants. The mRNA level was measured by RT-qPCR and data are expressed as relative to the WT samples. Data are mean ± SD of three-four biological replicates (Student't test, *P<0.05; **P<0.01).

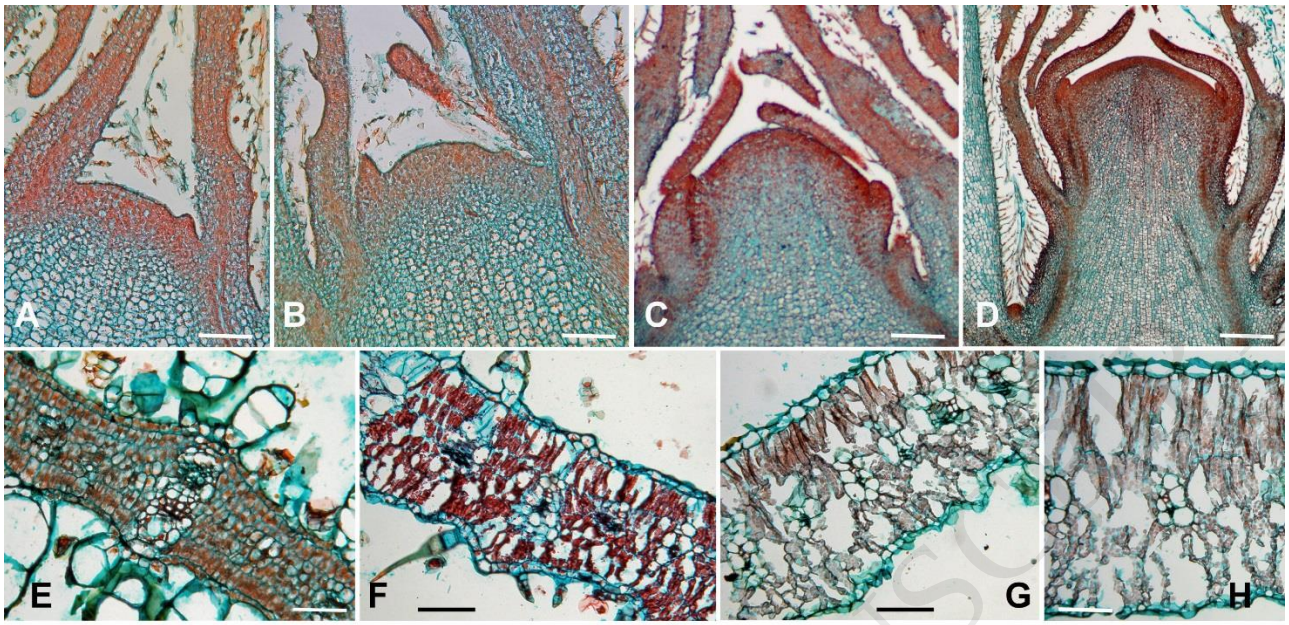

Fig. S1.

Fig. S1. Anatomical analysis in different explants of *linho* (*linho*/*linho*) and wild type (*LINHO*/*LINHO*; WT) plants during vegetative stage and at phase transition. (A) Longitudinal section of the *linho* shoot apical meristem (SAM) at vegetative stage. (B) Longitudinal section of the WT SAM at vegetative stage. (C) Longitudinal section of the *linho* SAM after vegetative-to-reproductive transition. (D) Longitudinal section of the WT SAM after vegetative-to-reproductive transition. (E) Longitudinal section of the *linho* leaf of phytomer below the inflorescence (with lamina folded down). (F) Longitudinal section of the WT leaf of phytomer below the inflorescence. (G) Longitudinal section of the *linho* leaf of fourth phytomer above cotyledons (with bullate lamina). (H) Longitudinal section of the WT leaf of fourth phytomer above cotyledons. Scale bar = 106 μm (A), 109 μm (B), 177 μm (C), 300 μm (D), 58 μm (E), 74 μm (F), 84 μm (G), 72 μm (H).

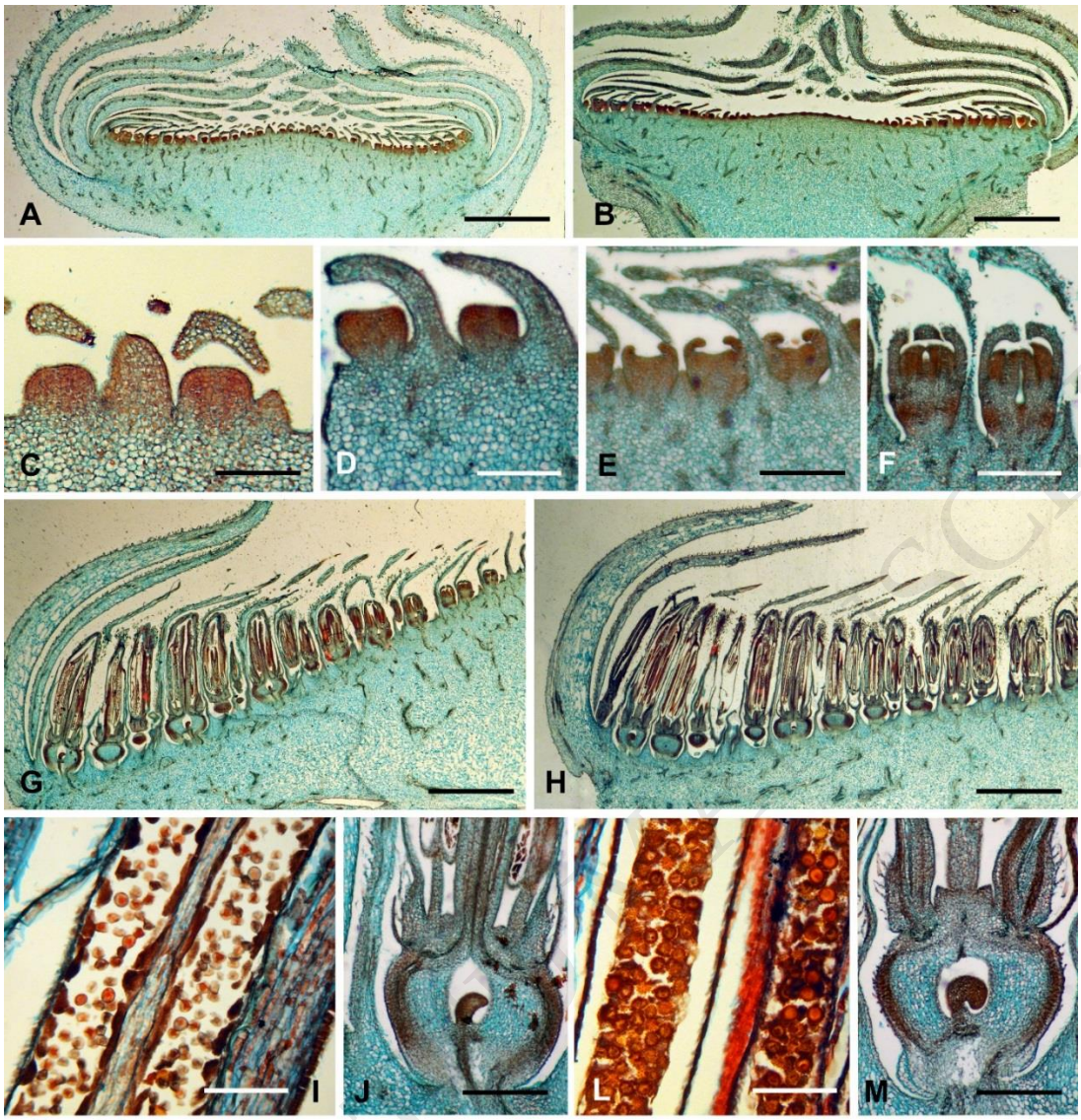

Fig. S2.

Fig. S2. Anatomical analysis in different explants of *linho* (*linho*/*linho*) and wild type (*LINHO*/*LINHO*; WT) plants during reproductive stage. (A-B) Longitudinal section of the *linho* (A) and WT (B) capitulum during early stage of development (diameter 1-1.5 cm). (C-F) Longitudinal sections of tubular flowers with progressive stages of development in the *linho* mutant. (G-H) Longitudinal section of the *linho* (G) and WT (H) inflorescence at later stage of development (diameter of 3-4 cm). (I) Longitudinal section of anthers in the *linho* inflorescence with 3-4 cm of diameter. (J) Longitudinal section of ovary in the *linho* inflorescence with 3-4 cm of diameter. (L) Longitudinal section of anthers in WT inflorescence with 3-4 cm of diameter. (M) Longitudinal

section of ovary in WT inflorescence with 3-4 cm of diameter. Scale bar = 1.440 mm (A), 1.251 mm (B), 139 μm (C), 193 μm (D), 245 μm (E), 303 μm (F), 1.812 mm (G), 2.40 mm (H), 92 μm (I), 379 μm (J), 99 μm (L), 395 μm (M).

Table 1

Inheritance of the *lingering hope* (*linho*) mutant of sunflower (*Helianthus annuus* L.). The mutant is sterile; therefore, the genetic analysis was conducted for three years, on heterozygous progenies.

Number of progenies	Phenotype and No. of plants. Genotypes are indicated in brackets		χ^2 (3:1)	*P*	Heterogeneity	
	Normal (*LINHO*/*LINHO*; *LINHO*/*linho*)	Mutant (*linho*/*linho*)			χ^2	*P*
10	738	269	1.572	0.20 - 0.30	6.168	0.70 - 0.80

Table 2

Plant height (cm) of wild type (*LINHO*/*LINHO*; WT) and *lingering hope* (*linho*/*linho*) mutant field-grown plants in two different reproductive stages. The data are means ± SE of three-four independent experiments (progenies), each with 50 replicates (plants). R3 and R6 stages according to Schneiter and Miller (1981). ** Significantly different from WT at the $P < 0.01$ level according to a Student's *t*-test.

Stage	WT	*linho*
R3	84.75 ± 0.970	33.57 ± 0.830 **
R6	121.73 ± 1.470	38.00 ± 1.120 **

Table 3

Pigment contents (μg mg^{-1} FW) of wild type (*LINHO*/*LINHO*: WT) and *lingering hope* (*linho*/*linho*) mutant potted plants grown under 200 μmol m^{-2} s^{-1}. Pigments were extracted from first and second pair of leaves. Data are means ± SE from three independent experiments, with samples run in triplicates (plants). ns: Not significant. *, ** Significantly different from WT at the $P < 0.05$ and $P < 0.01$ level according to a Student's *t*-test, respectively.

Pair of leaves	1st		2nd	
Genotype	WT	*linho*	WT	*linho*
Chl *a*	1.492 ± 0.022	1.079 ± 0.078 **	1.028 ± 0.058	0.629 ± 0.028 **
Chl *b*	0.436 ± 0.011	0.301 ± 0.014 **	0.346 ± 0.028	0.262 ± 0.017 *
Chl *a*+*b*	1.928 ± 0.032	1.379 ± 0.092 **	1.374 ± 0.085	0.892 ± 0.044 **
Car	0.391 ± 0.005	0.298 ± 0.011 **	0.356 ± 0.016	0.220 ± 0.006 **
Chl tot/Car	4.936 ± 0.073	4.608 ± 0.129 ns	3.845 ± 0.136	4.039 ± 0.137 ns
a/*b*	3.427 ± 0.038	3.574 ± 0.092 ns	3.019 ± 0.107	2.422 ± 0.068 **

Table 4

Gas exchange and fluorescence parameters of wild type (*LINHO*/*LINHO*: WT) and *lingering hope* (*linho*/*linho*) mutant potted plants grown under 200 μmol m^{-2} s^{-1} for three weeks. Values were obtained from first and second pair of leaves. Data are means ± SE from three independent experiments, with samples run in triplicates (plants). ns: Not significant. *, ** Significantly different from WT at the $P < 0.05$ and $P < 0.01$ level according to a Student's *t*-test, respectively.

Pair of leaves	First (1st)		Second (2nd)	
Genotypes	WT	*linho*	WT	*linho*
Gas exchange				
Parameters				
A (μmol m^{-2} s^{-1})	9.070 ± 0.650	8.070 ± 0.450 ns	9.060 ± 0.620	4.920 ± 0.450 **
g_s (mol m^{-2} s^{-1})	0.369 ± 0.050	0.301 ± 0.018 ns	0.347 ± 0.051	0.208 ± 0.013 ns
E (mmol m^{-2} s^{-1})	3.800 ± 0.400	3.250 ± 0.160 ns	4.320 ± 0.500	2.840 ± 0.110 *
C_i (μmol mol^{-1})	344.7 ± 3.700	342.3 ± 4.500 ns	344.3 ± 6.300	355.3 ± 5.400 ns
Fluorescence of Chl *a*				
Parameters				
Φ_{PSII}	0.723 ± 0.009	0.694 ± 0.026 ns	0.709 ± 0.011	0.555 ± 0.029 **
NPQ	0.087 ± 0.018	0.127 ± 0.007 ns	0.150 ± 0.036	0.170 ± 0.050 ns
F_v/F_m	0.788 ± 0.008	0.788 ± 0.007 ns	0.809 ± 0.006	0.705 ± 0.019 *

Table S1

Description of sunflower growth stages modified from Schneiter and Miller (1981).

Stage	Description	Note
VE	Seedling has emerged and the first leaf beyond the cotyledons is less than 4 cm long.	Vegetative emergence
V1, V2, V3 etc.	These are determined by counting the number of true leaves at least 4 cm in length beginning as V1, V2, V3, V4 etc.	Vegetative stages
R1	The terminal bud forms a miniature floral head rather than a cluster of leaves. When viewed from directly above the immature bracts form a many-pointed star-like pattern.	Reproductive stage
R2	The immature bud elongates from 0.5 to 2.0 cm above the nearest leaf attached to the stem. Disregard leaves attached directly to the back of the bud.	Reproductive stage
R3	The immature bud elongates more than 2.0 cm above the nearest leaf.	Reproductive stage
R4	The inflorescence begins to open. When viewed from directly above immature ray flowers are visible.	Reproductive stage
R5 (decimal)	This stage is the beginning of flowering. The stage can be divided into substages dependent upon the percent of the head area (disc flowers) that has completed or is in flowering. Ex. R5.3 (30%).	Reproductive stages
R6	Flowering is complete and the ray flowers are wilting.	Reproductive stage
R7	The back of the head has started to turn a pale yellow colour.	Reproductive stage
R8	The back of the head is yellow but the bracts remain green.	Reproductive stage

R9	The bracts become yellow and brown. This stage is regarded as physiological maturity.	Reproductive stage

References

Schneiter, A.A., Miller, J.F., 1981. Description of sunflower growth stages. Crop Sci. 21, 901-903

Table S2

List of genes analysed and gene-specific primers used for real-time RT-PCR (RT-qPCR). In square brackets are indicated the linkage groups of sunflower genome (Bodouin et al., 2017).

Gene	GenBank accession number	Primer	Primer sequence 5'-3'	Amplicon size (bp)
18S rRNA (*18S*) [1, 6, 12, 13, 14]	KF767534.1	18F 18R	Forward: TGACTCAACACGGGGAAAC Reverse: GACAAATCGCTCCACCAAC	120
Pathogenesis-related 5-1 (*PR5-1*) [17]	AF364864.1	PR5F PR5R	Forward: CCCTTCCCACTTTCCTTCTC Reverse: TGCGACGGTTAAAGACCAG	158
Defensin (*PDF 1.2*) [12]	AF364865.1	DEFF DEFR	Forward: CAATGCTTTTCTTCTGCTTCTC Reverse: TCACAGTGTTTTGTCTTGCC	123
UDP-glycosyltransferase 74G1-like (*SA GTase*) [9]	XM_022125270	UDPF UDPR	Forward: CCATCTACCTCAACTCTACCC Reverse: TATCTGCACTCGCGTAACC	105
Isochorismate synthase 2 (*ICS2*) [14]	OTF99857.1	ICSF ICSR	Forward: AGCAACATTTTCAGCATCTTCC Reverse: AAGACAGCAGAACCCAGACC	145

References

Badouin, H., Gouzy, J., Grassa, C.J., Murat, F., Staton, S.E., Cottret, L., Lelandais-Brière, C., Owens, G.L., Carrère, S., Mayjonade, B., Legrand, L., Gill, N., Kane, N.C., Bowers, J.E., Hubner, S., Bellec, A., Bérard, A., Bergès, H., Blanchet, N., Boniface, M.C., Brunel, D., Catrice, O, Chaidir, N., Claudel, C., Donnadieu, C, Faraut, T., Fievet, G., Helmstetter, N., King, M., Knapp, S.J., Lai, Z, Le Paslier, M.C., Lippi, Y., Lorenzon, L., Mandel, J.R., Marage, G., Marchand, G., Marquand, E., Bret-Mestries, E., Morien, E., Nambeesan, S., Nguyen, T., Pegot-Espagnet, P., Pouilly, N., Raftis, F., Sallet, E., Schiex, T., Thomas, J., Vandecasteele, C., Varès, D., Vear, F., Vautrin, S., Crespi, M., Mangin, B., Burke, J.M., Salse, J., Muños, S., Vincourt, P., Rieseberg, L.H., Langlade, N.B., 2017. The sunflower genome provides insights into oil metabolism, flowering and Asterid evolution. Nature 546, 148-152.

Table S3

Cell length (μm) in cross and longitudinal sections of eighth-ninth internode of wild type (*LINHO*/*LINHO*; WT) and *lingering hope* (*linho*/*linho*) mutant potted plants. Data are means ± SE of 5 internodes from 5 potted plants. ns: Not significant. * Significantly different from WT at the $P < 0.05$ level according to a Student's *t*-test.

Genotype	Cross sections		Longitudinal sections
	Parenchymal cells	Medullary cells	Parenchymal cells
WT	34.79 ± 4.04	62.76 ± 6.01	30.40 ± 2.30
linho	41.14 ± 1.30 *	65.31 ± 8.09 ns	31.28 ± 3.10 ns